Semiconductor–metal phase transition in rare-earth semiconductors (samarium monochalcogenides)

I. A. Smirnov and V. S. Oskotskiĭ

A. F. Ioffe Physicotechnical Institute, USSR Academy of Sciences, Leningrad

A review is given of the theoretical and experimental data on the isostructural first-order semiconductor–metal phase transition in samarium monosulfides and $Sm_{1-x}Ln_x^{3+}S$ solid solutions (Ln is a rare-earth metal). Phase transitions occurring under hydrostatic pressures and as a result of change in temperature are considered. Electrical, magnetic, galvanomagnetic, thermoelectric, thermal, optical and mechanical properties are discussed, as well as the energy band structure of the semiconductor and metal modifications of the investigated materials. Special attention is given to the experiments confirming the fractional valence of the samarium ion in the metal phase of these materials (the experimental evidence for this valence is provided by the Mössbauer effect, magnetic susceptibility, shifts of x-ray K lines, x-ray emission spectra, and specific heat).

PACS numbers: 72.60.+g, 71.25.Tn, 72.20.−i, 78.70.En

CONTENTS

1. INTRODUCTION. RARE-EARTH SEMICONDUCTORS—A NEW CLASS OF MATERIALS

A new class—rare-earth—of semiconductors, which includes the samarium chalcogenides considered in the present review, is currently attracting considerable interest. One must point out immediately that we are dealing here not with a quantitative accumulation of standard materials for investigation but with a basically new class of compounds. Many effects observed in these compounds have forced theoreticians and experimentalists to modify the usual points of view established in the course of investigations of standard semiconductors (such as Ge, Si, or III-V compounds, etc.).

A. Special properties of rare-earth semiconductors

1) A rare-earth semiconductor contains a rare-earth ion with a partly filled inner $4f$ shell. This shell gradually fills along the series from La to Lu[1] (second column in Table I).[1] The f levels are located deep inside an atom and are screened by the $5s^2p^6$ electrons from external perturbations. When a compound is formed, the f shells do not overlap one another (the radius of the $4f$ shell is ~0.3 Å, which represents ~0.1 of the interatomic distance) but form localized levels of density

~10^{22} cm^{-3}. The energies of these levels may lie within the forbidden band (band gap) of a semiconductor and can then act as "impurity levels." This is a unique feature because it has never been possible to attain such an enormous density of local impurity levels in standard semiconductors. When the $4f$ levels of a rare-earth semiconductor have energies inside the forbidden band,

TABLE I. Electron configurations of $4f$-element ions.

Ion	Electron configuration $(Xe)4f^n$	S	L	J	Ground term (lowest multiplet level)
La³⁺, Ce⁴⁺	$4f^0$	0	0	0	$^1S_0$
Ce³⁺	$4f^1$	1/2	3	5/2	$^2F_{5/2}$
Pr³⁺	$4f^2$	1	5	4	$^3H_4$
Nd³⁺	$4f^3$	3/2	6	9/2	$^4I_{9/2}$
Pm³⁺	$4f^4$	2	6	4	$^5I_4$
Sm³⁺	$4f^5$	5/2	5	5/2	$^6H_{5/2}$
Eu³⁺, Sm²⁺	$4f^6$	3	3	0	$^7F_0$
Gd³⁺, Eu²⁺	$4f^7$	7/2	0	7/2	$^8S_{7/2}$
Tb³⁺	$4f^8$	3	3	6	$^7F_6$
Dy³⁺	$4f^9$	5/2	5	15/2	$^6H_{15/2}$
Ho³⁺	$4f^{10}$	2	6	8	$^5I_8$
Er³⁺	$4f^{11}$	3/2	6	15/2	$^4I_{15/2}$
Tm³⁺	$4f^{12}$	1	5	6	$^3H_6$
Yb³⁺	$4f^{13}$	1/2	3	7/2	$^2F_{7/2}$
Lu³⁺, Yb²⁺	$4f^{14}$	0	0	0	$^1S_0$

---

[1] Table I gives also the quantum numbers L, S, and J representing the orbital, spin, and total angular momenta, as well as the symbols for the lower level of the term in question.

these levels dominate the transport phenomena and optical properties, give rise to various phase transitions, etc.

2) The presence of ions with partly filled $4f$ shells in rare-earth semiconductors is responsible for the lack of compensation of the spin and orbital angular momenta. The appearance of magnetic ordering may be expected for these compounds. However, the presence of partly filled shells is a necessary but not a sufficient condition for magnetic ordering. Therefore, not all rare-earth semiconductors are also magnetic materials.

3) The conduction band of a rare-earth semiconductor is formed from the s and d electrons (the valence electrons in rare-earth metals are $5d^16s^2$). The formation of compounds may give rise to narrow allowed d-bands. There may be cases when the $4f$ levels are "dislodged" to the d band; in this case, the f-d exchange interaction may transform them into a very narrow ($\sim 10^{-1}$-10^{-2} eV) band. The presence of narrow bands requires the development of a new theory and forces the abandonment of a number of assumptions in the standard theory of semiconductors (energy band spectrum, assumption of weak electron–electron correlation, hypothesis of the validity of the transport equation, etc.[2]).

It follows that investigations of rare-earth semiconductors present a number of problems.

B. Type of material belonging to rare-earth semiconductors

The rare-earth elements (including yttrium and scandium) represent over 16% of all the elements known at present. Combinations of rare earths with other elements in the Mendeleev table give an enormous number of all kinds of compounds, some of which are semiconductors. Semiconductor properties are exhibited by chalcogenide series of the LnX, Ln_2X_3, Ln_3X_4 and more complex types (here, Ln is a rare-earth element and X is O, S, Se, or Te), and by some borides. In principle, pnictides LnB (B is N, P, As, Sb, or Bi) should be narrow-gap semiconductors.[2] Wide-gap semiconductors include halides (LnC_3, LnC_2, etc., where C is F, Cl, Br, or I), oxychalcogenides (Ln_2O_2X), rare-earth orthoferrites ($LnFeO_3$), and iron garnets ($Ln_3Fe_5O_{12}$). There are many complex (ternary, quaternary) semiconductor compounds formed from rare-earth and $3d$ elements. Of the compounds which exhibit all three characteristic features of rare-earth semiconductors, the most thoroughly investigated at present are the rare-earth monochalcogenides LnX (X is S, Se, Te, and O but only in the case of EuO; Ln is Sm, Eu, or Yb). All the LnX monochalcogenides crystallize in the NaCl structure and, depending on the
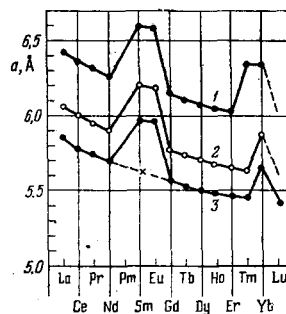
FIG. 1. Dependence of the lattice constant of LnTe (1), LnSe (2), and LnS (3) compounds on the atomic number of the rare-earth element.[1]

valence state of the rare-earth ion, can be either metals or semiconductors (metals when the rare-earth ion is trivalent and semiconductors when it is divalent). Since the Sm, Eu, and Yb ions (and—in some compounds—Tm ions) are divalent in the stable state, their monochalcogenides are semiconductors.

Figure 1 shows the dependence of the lattice period a of LnX on the atomic number of the rare-earth element.[1] An increase in the atomic number of the trivalent rare-earth element is accompanied by a monotonic fall in a because of the lanthanoid compression of the cation. The lattice constants of the monochalcogenides of the divalent rare earths (Sm, Eu, Yb, Tm) depart from this monotonic dependence, forming sharp maxima. The greatest amount of work has been done recently on the EuX monochalcogenides.

Europium monochalcogenides are magnetic semiconductors and have a number of unique properties. The oxide EuO exhibits a low-temperature (near 50 °K) insulator–metal phase transition which alters the electrical conductivity by 15 orders of magnitude, and the EuX monochalcogenide group as a whole is characterized by a giant magnetoresistance (up to 10^6) near the magnetic ordering temperatures and a high absolute red shift of the absorption edge. Doping the EuX monochalcogenides alters their electrical properties and, conseqently, changes greatly the magnetic characteristics; moreover, giant magnetooptic effects are observed. These materials exhibit pure Heisenberg magnetism and simple crystal lattices, and this facilitates theoretical calculations. Over 200 papers have been published already on europium monochalcogenides. Readers interested in fuller details of these compounds are directed to the published reviews.[1,3-6]

Less work has been done on ytterbium and thulium monochalcogenides. Samarium monochalcogenides will be considered in the present review.

2. REASONS FOR INTEREST IN SAMARIUM MONOCHALCOGENIDES

In the last five years, samarium monochalcogenides (particularly SmS) have attracted the attention of many investigators. This increased interest is due to a number of factors.

1) The "self-doping" effect in rare-earth semiconductors, mentioned in the preceding section, was first discovered in the semiconductor modifications of SmX

---

[2] Because of the difficulties in synthesis and the insufficient purity of the starting rare-earth metals, it has not yet been possible to prepare samples of LnB with semiconductor properties.

I. A. Smirnov and V. S. Oskotskiĭ   118

(X is S, Se, or Te). The $4f$ levels of samarium mono-chalcogenides lie close to the conduction band and act as donor impurities.[1,7-14]

2) It has been found that SmS has a wide homogeneity range within which its physical properties may vary from those typical of semiconductors to semimet-als.[10,14,15]

3) The SmX monochalcogenides may be regarded as "magnetoexciton" semiconductors.[16] This class of materials has $J = 0$ in the ground state (see Table I) but the energy of its transition to the state with a finite J (for example, $J = 1$) is low.[17-21]

4) In 1970, Jayaraman et al.[22] discovered an iso-structural (NaCl–NaCl) first-order semiconductor–metal transition in SmS subjected to a hydrostatic pressure of $P_{cr} = 6.5$ kbar (300 °K). The low absolute value of the critical pressure P_{cr} and the retention of the crystal lattice type after the transition are very rare in solid-state physics.

5) In contrast to SmS, both SmTe and SmSe go over to the metal modification under hydrostatic pressure not abruptly but gradually. The type of crystal struc-ture is retained but "metallization" occurs at fairly high pressures (~ 60 kbar for SmTe and ~ 50 kbar for SmSe[23]).

6) It has been found that the metal modification of samarium monosulfide, obtained at pressures $P_{cr} \geqslant 6.5$ kbar (we shall call it the high-pressure phase) has unusual properties and is completely dissimilar from neighboring metals which are rare-earth mono-sulfides. Consequently, this monosulfide (together with certain other materials) can be assigned to a sepa-rate class of metals whose principal distinguishing characteristic is the fractional valence of the rare-earth ion.

The unusual nature of the phase transition in SmS under hydrostatic compression and the possibility of the fractional valence of the rare-earth ion have trig-gered off an avalanche of theoretical papers[24-80] at-tempting to construct a model of this phase transition and to explain the very unusual experimental results. The leading Soviet (Ioffe Physicotechnical Institute, Leningrad) and non-Soviet (IBM and Bell Laboratories, USA, Solid-State Physics Institute in Zurich, etc.) research establishments have joined the research ef-fort. A very large amount of experimental data has now been accumulated. Attempts at the partial sys-tematization of these data (at various stages of the re-search) have been made.[23,62,75,81-84] A common short-coming of these limited reviews has been the concen-tration on some specific effects or summing up of the work done only in the authors' own laboratory.

We shall consider two topics:

1) the semiconductor–metal phase transition in SmX, and

2) the fractional valence of the Sm ion in the metal modification of these compounds.

We shall be interested in the experimental work and

in the theoretical interpretations. We shall need: a) to know the main parameters and the energy band struc-ture of the semiconductor and metal modifications of SmS; b) to review the data obtained at the phase transi-tion point or in its direct vicinity; and c) to discuss the experimental results confirming the fractional valence of the Sm ion in the metal phase. We shall follow this scheme in our review. Investigations of the semicon-ductor–metal phase transition in samarium mono-chalcogenides have revealed that the metal modification can be obtained not only by hydrostatic pressure (but also by other methods). Therefore, before considering the basic experimental data, we shall briefly review the methods used to prepare the metal modification of SmX.

3. METHODS FOR PREPARATION OF THE METAL MODIFICATIONS OF SmX

At present, we know of one method (No. 1) for ob-taining the metal modifications of SmTe and SmSe and three methods (Nos. 1, 2, and 3) for SmS.

The first method involves the use of hydrostatic pres-sures exceeding $P_{cr} = 6.5$, 50, and 60 kbar for SmS, SmSe, and SmTe, respectively.[20,21,82-99] Since the trivalent samarium ion has a smaller radius (r_i) than the divalent ion ($r_i = 1.14$ Å for Sm^{2+} and 0.96 Å for Sm^{3+}[75]), it is natural to expect that hydrostatic pres-sure can produce the $Sm^{2+} \to Sm^{3+}$ transition and the high-pressure metal phase.[3] The advantage of this method is its ability to produce the metal modification in fairly large volume. Its disadvantages are as follows:
a) studies of the physical properties have to be carried out in special bombs at high hydrostatic pressures;
b) removal of the pressure results in fracture of the sample during the reverse metal–semiconductor transi-tion (see Sec. 4).

The second method involves mechanical polishing of thin films of the semiconductor modification of SmS.[100-116] This method was developed at the Ioffe Physicotechnical Institute in 1974.[100] The history of this method is as follows. In 1964, some investigators at the Institute[9] discovered an interesting effect (also observed by others later[22,117-123]): polishing (and, in the case of a freshly cleaved surface, even light touch-ing with a finger) single-crystal and polycrystalline samples of the semiconductor phase of SmS altered its black surface to a golden-yellow color. The optical re-flection data[1,120] indicated that this procedure produced a thin surface layer of the metal phase of SmS. This layer retained its properties indefinitely at atmospheric

---

[3] The isostructural (NaCl–NaCl) semiconductor–metal phase transition in LnX under hydrostatic compression occurs also in the case of other divalent rare-earth ions. The value of P_{cr} for YbTe, YbSe, and YbS is $\sim 150-200$ kbar, and that for EuO is ~ 300 kbar. In the case of TmTe there is a gradual transition in the 1–40 kbar range. Up to pressures cor-responding to the transition to the metal phase the europium chalcogenides EuTe, EuSe, and EuS exhibit the NaCl–CsCl structural transition at ~ 110, ~ 145, and ~ 215 kbar, re-spectively.[23,81]

pressure and room temperature. However, it was difficult to investigate its physical properties (apart from the reflection coefficient) because of the shunting effect of the relatively thick semiconductor substrate. The metal modification of SmS, stable at atmospheric pressure, was first produced in 1974[100] by polishing thin semiconductor films of samarium monosulfide. This metal phase was created throughout the film.[4] This was confirmed by x-ray investigations and visually: the film was golden-yellow on the free and substrate sides. Such a film could be converted back to the semiconductor phase by heating to 200–300 °C.

The advantage of this method is the feasibility of preparing samples of the metal modification of SmS stable at atmospheric pressure in the temperature range $T < 200$–300 °C. The disadvantages of the method are that a) the metal modification is obtained in the form of a thin film representing a small amount of the material and b) some physical measurements give somewhat indeterminate results because of the presence of the substrate on which the film is evaporated.

The third method involves the formation of solid solutions of trivalent rare-earth monosulfides in SmS. [81–84,124–155]

This method can be used to prepare the metal modification stable at atmospheric pressure. The first experiments were carried out in 1973 by Jayaraman *et al.*[124] on the $Sm_{1-x}Gd_xS$ system. The idea of the method was as follows: the lattice constant of GdS (5.563 Å) was known to be considerably smaller than that of SmS (5.97 Å) so that the replacement of Sm with Gd should result in lattice compression, equivalent to the application of hydrostatic pressure to the Sm sublattice. This produced an "internal lattice pressure" in the crystal and, for a certain critical value of the lattice constant $a_{cr} \approx 5.7$ Å (corresponding to the ~ 15 at.% Gd concentration) could initiate the isomorphous semiconductor–metal transition in $Sm_{1-x}Gd_xS$ (this effect is sometimes known in the literature as the "chemical collapse"). Gadolinium stablilizes the SmS metal phase at atmospheric pressure. Subsequently, the elements La, Ce, Pr, Nd, Tb, Dy, Ho, Er, Tm, Lu, and Y were used as the "lattice press." It has been found that chemical collapse is possible not only as a result of the formation of solid solutions with $Ln^{3+}S$ but also on the replacement of Sm with the quadrivalent Th ion ($Sm_{1-x}Th_xS$) and the replacement of S with arsenic ($SmS_{1-x}As_x$). The advantage of the method is the feasibility of obtaining the metal modification of SmS stable at atmospheric pressure but its disadvantage is the difficulty of interpreting the experimental results because of the presence of a considerable "background" due to the presence of a high concentration of Ln^{3+} or other ions acting as the "lattice press."

In all the above three methods, the phase transition is due to hydrostatic compression. The situation is a little more complex in the case of retention of the metal modification at atmospheric pressure in the second method. [156]

Subsequent experiments (see Sec. 4) have shown that the metal modifications of SmS produced by the first and second methods are completely identical. The metal modification resulting from the formation of solid solutions has certain special features. Apparently, the role of Ln^{3+} and other ions is not limited to their action as the "press." Moreover, a necessary condition for the collapse is the identity of the energy band structure of the dopant and SmS. This has made it possible to consider solid solutions based on SmS as a special class of materials which will be discussed in Sec. 5.

4. SAMARIUM MONOCHALCOGENIDES

A. Semiconductor modification

A model of the semiconductor–metal phase transition in SmX can be constructed if we know the energy band structure of the compound in question before and after the phase transition.

The most interesting and sufficiently thoroughly investigated material among samarium monochalcogenides is SmS. The present review will be mainly concerned with its properties. Samarium sulfide crystallizes in the NaCl structure and, at 300 °K, its lattice constant is 5.97 Å, which is close to the sum of the ionic diameters of the cation and anion (the ionic radii in angstroms are 1.14 for Sm^{2+} and 1.84 for S^{2-}).[5] Before considering the available data on the energy band structure of the semiconductor phase of SmS, we shall deal with at least two of its special properties that have to be allowed for in the interpretation of the experimental results.

1) As pointed out in Sec. 1, SmS has a wide homogeneity range which extends from 50 to 54 at.% Sm but does not extend in the direction of excess sulfur, i.e., SmS is a unilateral unlimited variable-composition phase. A comparison of the experimental and calculated densities shows that the excess samarium occupies interstices of the crystal lattice (at the same time, a certain number of vacancies appears in the sulfur sublattice). Samarium sulfide always has n-type conduction. Within the limits of its homogeneity range, there is a variation from semiconductor to metal properties. [1,10,14,15,157][6]

2) The presence of an adjacent first multiplet of SmS with $J = 1$[19,20,158] has a considerable influence on the magnetic susceptibility,[17,18,159] optical properties,[144,147,148] specific heat,[160,161] and transport coefficients.[157]

---

[4] The metal modification can be produced by polishing in films up to 0.5 μ thick, and by combination of polishing and uniaxial pressure in films up to 1–2 μ thick.

[5] The compounds SmSe and SmTe have lattice constants of 6.22 and 6.60 Å, respectively, and ionic radii of Se^{2-} and Te^{2-} in these compounds are 1.98 and 2.21 Å.[75]

[6] The carrier density in the homogeneity region varies from $\sim 10^{19}$ to $\sim 10^{20}$ cm^{-3}; there are large changes in the thermal characteristics, lattice constant, and density; the color of the sample remains black. [1,10,14,15]
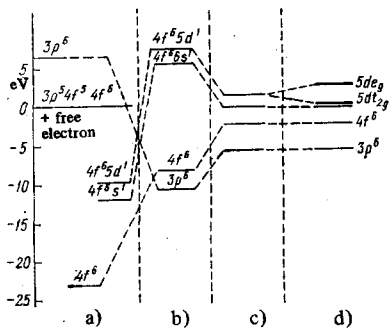
FIG. 2. Energy levels of electrons in SmS[84,120]: a) free ions; b) crystal with allowance for the Madelung energy; c) crystal with allowance for the Madelung and polarization energies; d) crystal with allowance for the Madelung and polarization energies, and for splitting of the d states in the crystal field.

The energy band structure of samarium monochalcogenides has been considered by applying the Born–Haber method to crystalline SmS on the basis of the experimental data for free samarium and sulfur ions[84,120] (Fig. 2). Unfortunately, this theory only gives a qualitative picture of the energy band structure and does not tell us which of the subbands (that formed by the $5d$ or $6s$ states) is lower on the energy scale and what is the absolute gap $(\mathscr{E}_g)$ between the $4f$ levels and the conduction band edge. In the first approximation, this information can be obtained only from an analysis of the experimental results on the transport phenomena. The absolute value and temperature dependence of the Lorenz number, deduced from the electron component of the termal conductivity,[162,163] definitely show that the s band of SmS is located lower on the energy scale than the d band. The temperature dependences (in the range 80–1000 °K) of the electrical conductivity σ, Hall coefficient R_H[1,7–10,14,157] magnetic susceptibility,[164] and electron component of the thermal conductivity[162] indicate that $\mathscr{E}_g$ of SmS is ~0.23–0.25 eV.[7]

Thus, the conduction band of the semiconductor modification can be represented as shown in Fig. 3. Figure 3 is a schematic diagram of the conduction band of $Sm_{1.015}S$ at $T = 500 °K$.[162] This model applies throughout the homogeneity range of samarium monosulfide, except that, for compositions close to stoichiometry, the Fermi level is in the s band and approaches the bottom of the d band only at temperatures $T \geqslant 100 °K$. The density-of-states effective masses in the s and d bands are $m_s^* = 0.78m_0$ and $m_d^* = 1.4m_0$[1,162] and the forbidden band width ΔE_g, representing the band gap between the valence $(3p)$ and conduction bands (Fig. 2) is ≈ 2.3 eV.[112,120]

It should be pointed out that in the case of the semiconductor modification of SmS with the band structure shown in Fig. 3 it is impossible to determine $\mathscr{E}_g$ by simple optical measurements because the $f–s$ transi-

tions are forbidden by the selection rules since the orbital quantum number then changes by 3.

It is worth considering specially the interpretation of the numerous optical data obtained for SmX[81,83,92,94,108,111–120,122,123,131–133,165–179] because they reveal a special feature of ionic rare-earth semiconductors: the optical data association with the $f–d$ transitions cannot be used in determing the energy band structures of these compounds.

The optical absorption spectrum of SmS reveals the localized atomic nature of the f electrons. The initial (ground) state has the $4f^6$ configuration with $L = 3$, $S = 3$, $J = 0$, i.e., $4f^6(^7F_0)$ (see Table I). One of the f electrons is excited optically to a higher energy state. In a free atom, this is the $5d$ state. In an SmS crystal, the crystal field splits the $5d$ state into a lower triply degenerate t_{2g} level and a higher doubly degenerate e_g level. We shall now consider where the remaining $5f$ electrons are located.

Since the total momentum of one f electron is $5/2$ or $7/2$, it follows that, after removal of one electron from the $4f^6$ shell, characterized by $J = 0$, the remaining $5f$ electrons are characterized by $J = 5/2$ and $7/2$.

The value of L for the remaining $4f^5$ shell should be such that the total parity of this shell and of the electron transferred to the d state is the same as for the odd $4f^6(^7F_0)$ state, i.e., the $4f^5$ state should be odd and L should assume only the odd values 5, 3, or 1. According to the Hund rule, the energy of the state with $L = 5$ is the lowest and it should be followed by the states with $L = 3$ and $L = 1$. Thus, the final states in the $4f^5$ shell after optical excitation of one electron may be, in increasing order of their energy: $4f^5(^6H)$, $4f^5(^6F)$, $4f^5(^6P)$, the separation between the first and second level amounting to 1 eV, and that between the second and third being 2.25 eV.[180] Thus, the final states of a system of five f electrons and an excited d electron may be as follows: $4f^5(^6H)5d(t_{2g})$, $4f^5(^6H)5d(e_g)$, $4f^5(^6F)5d(t_{2g})$, $4f^5(^6F)5d(e_g)$, $4f^5(^6P)5d(t_{2g})$, and $4f^5(^6P)5d(e_g)$. We shall use this information to analyze the optical absorption spectra of SmS, SmSe, and SmTe. These spectra are shown in Fig. 4. The localized $4f$ shells of the samarium ion in the three compounds should be practically identical, and the crystal splitting between the t_{2g} and e_g states should depend on the lattice constant a. Therefore, the separations between the peaks of the transitions to

FIG. 3. Schematic representation of the conduction band of the semiconductor modification of SmS.[162] The data are given for a sample of $Sm_{1.015}S$ at $T = 500 °K$ with the following parameters: $\Delta = 0.08$ eV, $\mathscr{E}_2 = 0.1$ eV, and $\mathscr{E}_1 \sim 0.09$ eV[162]; the levels $\mathscr{E}_1$ are associated with the presence of impurities.

---

[7] In the case of SmSe and SmTe, approximate estimates give values of $\mathscr{E}_g$ of 0.5 and 0.7 eV, respectively.[81] There is no published information on the relative positions of the s and d subbands in these compounds.
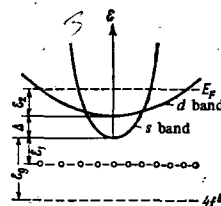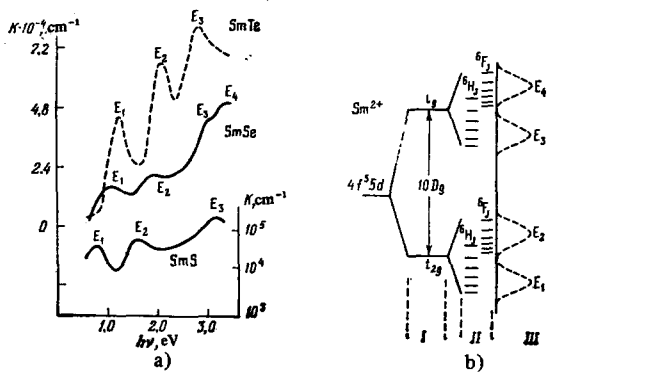
FIG. 4. a) Absorption spectra of SmTe, SmSe, and SmS[1] at 300 °K. b) Schematic representation of the splitting of the 5d levels of Sm^{2+} by the crystal field: I) influence of the cubic crystal field on the 5d levels; II) splitting of the 4f^5 multiplets; III) observed absorption peaks. [81]

FIG. 5. a) Dependences $\rho(P)$ for SmS, SmSe, and SmTe. [23] b) Dependence of the electrical resistance on P for SmS[22] at 300 °K.

states with the same d levels but different 4f^5 levels should be identical for all the crystals and the separations between the transitions to states with the same 4f^5 levels but different d levels should decrease with increase in the lattice constant. It is clear from Fig. 4 that E_1, E_2, and E_3, E_4 form pairs with the same differences $E_2 - E_1$ and $E_4 - E_3$, amounting to ~1 eV for all the crystals, but the separation between the pairs should decrease rapidly with increase in the lattice constant. It follows from this analysis that E_1 corresponds to a transition from the state 4f^6($^7F_0$) to the state 4f^5(^6H)5d(t_{2g}), E_2 corresponds to a transition to the state 4f^5(^6F)5d(t_{2g}), E_3 to 4f^5(^6H)5d(e_g), and E_4 to 4f^5(^6F)5d(e_g). The splitting of the levels e_g and t_{2g} in SmS is ~2.3 eV.

Thus, the f levels are definitely of atomic nature and little affected by the crystal environment.

We shall now consider the nature of the optically excited d states in an SmS crystal. Although the f-electron energy is close to the bottom of the conduction band, the f electrons cannot be regarded as ordinary shallow donors because the wave function of an f electron is very strongly localized, has the momentum $l = 3$, and in no way resembles the hydrogen-like wave function of an electron with $l = 0$ localized at a shallow donor level. This also applies to an excited d electron: it is localized in a region of atomic size and has $l = 2$. Therefore, the usual picture of the optical excitation of hydrogen-like donor levels or of the ionization of donors accompanied by the transfer of an electron to the conduction band is inapplicable. An excited d state is strongly coupled to its own ion and is of an exciton nature. Its energy lies well above the bottom of the conduction band ($E_1 \approx 0.8$ eV). The excitation is of a nonequilibrium nature because optical excitation of the Sm ion does not provide sufficient time for a change in the lattice. (It is interesting to note similar optical absorption spectra of the Sm^{2+} ion in CaF$_2$, SrF$_2$, and BaF$_2$ crystals,[181] which differ mainly by the crystal-field splitting.) Hence, we may conclude that the nature of the spectrum under consideration is not governed by transitions to the conduction band of the crys-
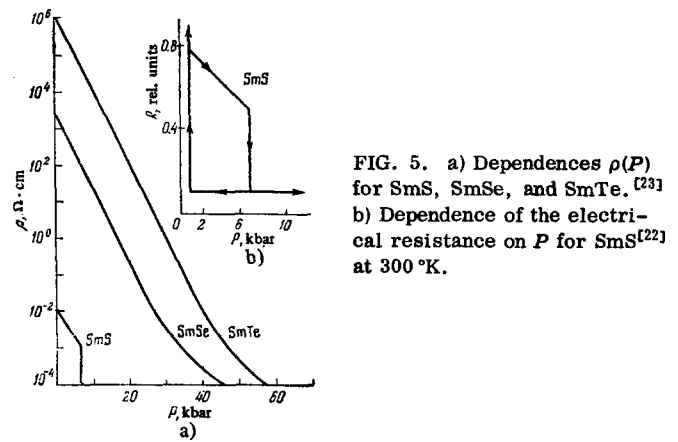
tal but by the excitation of excitons which largely retain the properties of atomic states.

The absorption peaks of SmS considered here are fairly wide, of the order of 1 eV. Clearly, this width represents the excited state and it is governed by a number of factors, including the overlap with the same states at the neighboring samarium ions. An exciton of this kind can move across a crystal but does not carry a charge. However, the dissociation of this exciton may result in the transfer of an electron to the conduction band, which—as pointed out above—is formed from the 4f^{6}6s and 4f^{6}5d states (i.e., an electron, roughly speaking, is transferred to a neighboring Sm ion as an additional particle). This results in charge transport, i.e., photoconductivity is exhibited. The states in the 4f^{6}6s band differ, in principle, from the optically excited states 4f^{5}5d not only because the excited electrons are different but also the f shells are different. A conduction electron in SmS, provided by an impurity or as a result of thermal excitation from the 4f^6 shell, travels through the crystal in the 4f^{6}6s band because it is not linked to its original site. This is the difference between a conduction electron and an optically excited exciton-type 4f^{5}5d state.

B. Semiconductor–metal phase transition

Figures 5–11 give some of the experimental data obtained for the semiconductor–metal phase transition in samarium monosulfide under the action of hydrostatic pressure. We shall now consider certain features of these data.
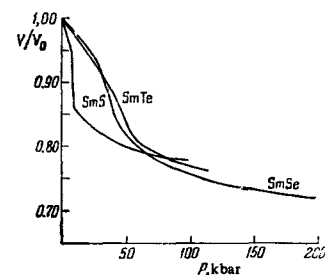

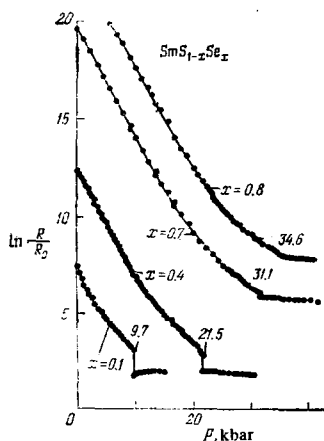FIG. 6. Dependences of V/V_0 on P for SmS, SmSe, and SmTe.

FIG. 7. Dependences of the relative electrical resistance on P for the $SmS_{1-x}Se_x$ solid solution system[182] at 300 °K.
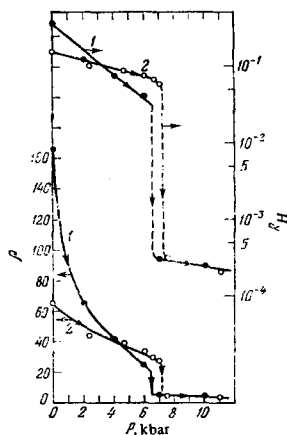
FIG. 8. Dependences of ρ and R_H on P for SmS single crystals: 1) composition close to stoichiometric; 2) samarium content ~50.2 at.%, 300 °K (only the dependences obtained under rising pressures are given).[97] Here, ρ is in units of 10^{-4} $\Omega \cdot cm$ and R_H is in units of cm^3/C.

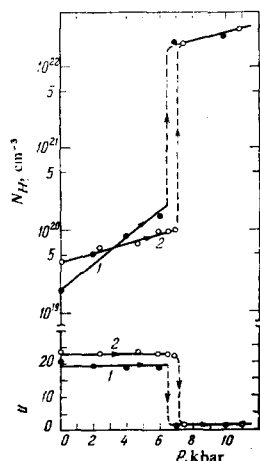FIG. 9. Dependences of the carrier mobility u and density N_H in SmS crystals on P[97]: 1), 2) same samples as in Fig. 8 (300 °K). Here, u is in units of $cm^2 \cdot V^{-1} \cdot sec^{-1}$.
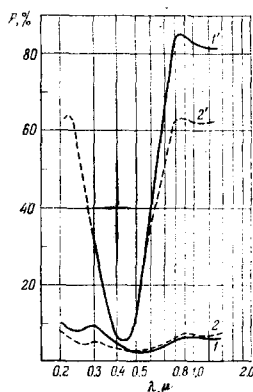
FIG. 10. Wavelength dependences of the optical reflection coefficient R of SmS (300 °K): 1), 1') bulk samples[92,94]; 1') measurements carried out under a hydrostatic pressure of 8 kbar; 2), 2') films.[101] Curves 1 and 2 represent the semiconductor phase and curves 1' and 2' the metal phase; in the case of curve 2' the metal phase was obtained by mechanical polishing of a semiconductor film 2.

1) The transition from the semiconductor to the metal modification under hydrostatic pressure is abrupt in SmS and gradual in SmTe and SmSe (Figs. 5 and 6).

2) Solid solutions of the $SmS_{1-x}Se_x$ type exhibit a gradual change from the abrupt to continuous phase transition[187] (Fig. 7). The value of P_{cr} rises almost linearly with the selenium concentration and the resistance discontinuity at P_{cr} decreases, tending to 0 at $x = 0.8$.

3) The resistivity ρ of the metal phase of all the SmX compounds is ~10^{-4} $\Omega \cdot cm$.

4) The phase transition alters the color of the samples (Table II). The process of phase transition under pressure in SmS has been followed visually under a microscope.[94] At 6 kbar, the "yellow spots" of the metal phase are still isolated but, at 6.5 kbar, the whole crystal becomes golden-yellow.

5) An anomalously large change in volume occurs on transition from the semiconductor to metal modification.

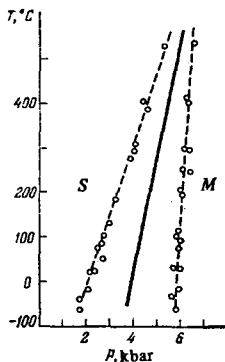6) The absolute value of the carrier mobility in Sms, deduced from R_H/ρ, is 20–25 and ~1 $cm^2 \cdot V^{-1} \cdot sec^{-1}$

FIG. 11. Temperature–pressure phase diagram of SmS.[98] Here, S is the semiconductor phase and M is the metal phase.

TABLE II.

Compound	Semiconductor phase	High-pressure metal phase
SmS	Black	Golden-yellow
SmSe	Black with bluish tinge	Bright copper
SmTe	Gray	Purple

TABLE III. Physical properties of semiconductor and metal phases of SmS.

Physical property	Semiconductor phase	Metal phase
Type of structure	NaCl	NaCl
Lattice constant, Å	5.97	5.70
Typical value of $\sigma_{300\,°K}$, $\Omega^{-1} \cdot cm^{-1}$	~20—30 (stoichiometric composition)	~10^4
Electron density at 300 °K, cm^{-3}	~10^{19} (stoichiometric composition)	~10^{22}
Color	Black	Golden-yellow
Forbidden band width ΔE_g, eV (gap between valence and conduction bands)	2.3	—
Separation between $4f$ levels and bottom of s conduction band $\mathscr{E}_g$, eV	~0.23 + 0.25	—
Carrier mobility at 300 °K, $cm^2 \cdot V^{-1} \cdot sec^{-1}$	20—25	~1
Bulk modulus, kbar	~475	~1100
References to the papers from which these properties are taken can be found in the text.		

for the semiconductor and metal phases, respectively (Figs. 8 and 9). In each phase, the mobility is constant and independent of the applied hydrostatic pressure. Hence, we may conclude that the fall in ρ with rising pressure (Fig. 8) in the semiconductor phase (up to the transition point) is entirely due to an increase in the carrier density. This allows us to calculate the value of $d\mathscr{E}_g/dP$. For sample No. 1, whose composition is close to the stoichiometric (Fig. 8), it amounts to ~ −10 meV/kbar. The value of $d\mathscr{E}_g/dP$ is less for sample No. 2 with excess Sm (Fig. 8).

7) The carrier density in SmS changes at the phase transition point from ~ 10^{20} to ~ 10^{22} cm^{-3} (Fig. 9).

8) In the homogeneity range of samarium monosulfide, an increase in the excess samarium concentration is accompanied by an increase in the absolute hydrostatic pressure at which the phase transition takes place (Fig. 8). This effect may be attributed to an increase in the lattice constant observed in the homogeneity range of Sms. [10,14,15]

9) The sign of the thermo-emf changes from negative to positive at the phase transition in SmS. [95]

10) The dependences of ρ, magnetic susceptibility χ, and reflection coefficient R on the pressure P exhibit a hysteresis on the removal of pressure (Fig. 5b). The reverse transition to the semiconductor modification occurs at 1.5-2 kbar and is accompanied by a considerable increase in volume, which frequently results in fracture of the sample.

11) The hysteresis effects become weaker at higher temperatures (Fig. 11). Linear extrapolation for the stoichiometric material gives zero hysteresis at 670–730 °C and a pressure of ~ 6.8 kbar. [98]

An analysis of the experimental data (constancy of

the structure before and after the phase transition, weakening of the hysteresis of the transition with rising temperature, and anomalously high compressibility of the semiconductor phase) led Tonkov and Aptekar'[98] to the conclusion of the existence, above 700 °C, of a critical point of the liquid–vapor type in the T–P phase diagram of SmS.[8]

The generally accepted description of the semiconductor–metal phase transition in SmX compounds under pressure is[82]

$$\text{Sm}^{2+} (4f^6;\ J = 0) \xrightarrow{P} \text{Sm}^{3+} (4f^5;\ J = 5/2) + e^- (d, s).$$
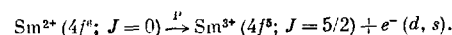
A theoretical model of this transition in SmS, SmSe, and SmTe will be discussed in detail in Sec. 6. We shall conclude the present subsection with Table III, which summarizes the main properties of the semiconductor and metal modifications of SmS.

C. Metal modification. Experimental data confirming fractional valence of the Sm ion

Figures 12–19 give some of the experimental results obtained for the metal modification of Sms. [9] Careful examination of these results is sufficient to show that the metal phase of SmS differs basically from similar metallic nonsulfides of trivalent rare earths. The dif-

---

[8] Before SmS, only one example of the T–P phase diagram with a critical point in the solid state has been known: this is the diagram showing the γ–α transition in Ce. [96]

[9] It is worth noting the full identity of the metal modifications of SmS prepared by hydrostatic compression and polishing of thin semiconductor films (see, for example, Fig. 10). In both cases the lattice constant is 5.7 Å, the temperature dependences of the electrical resistivity ρ and its absolute values are similar.
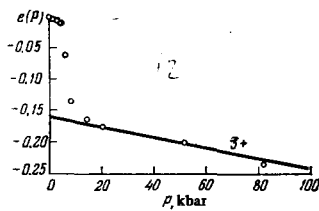
FIG. 12. Dependence of e on P for SmS[82] at 300 °K.

FIG. 13. Temperature dependences of the magnetic suscepti- bility[159]: 1) SmS; 2) SmSe; 3) SmTe; 4) SmS (under a hydro- static pressure of 6 kbar); 5) SmS ($P \sim 7.5$–12 kbar); 6) Sm_2In_3.

ferences are discussed below.

1) *Crystal lattice constant and* $\Delta V/V_0 = f(P)$. The lattice constant of the semiconductor phase of $Sm^{2+}S$ is 5.97 Å. Extrapolation of the dependence of the lattice constant a on the atomic number of the rare earth in the $Ln^{3+}S$ series between the nearest neighbors SmS, NdS, and GdS (dashed line in Fig. 1) gives the lattice constant 5.62 Å (denoted by a cross in Fig. 1) for the hypothetical metal modification $Sm^{3+}S$. The experi- mental value of a for the high-pressure phase of SmS ($P \sim 6.5$–10 kbar) is 5.7 Å. [22,100] Thus, we may as- sume that, in the high-pressure phase, the samarium ion has some intermediate valence between +2 and + 3.

An increase in the hydrostatic pressure ($P > 20$ kbar) causes the valence of Sm in Sm monosulfide to ap- proach gradually +3 (Fig. 12).[82,183] Figure 12 shows the dependence of the relative volume change e on the pressure $P[e = \Delta V/V_0 \approx 3\Delta a/a_0$, where Δa is the deviation of the lattice constant from the value a_0 obtained at at- mospheric pressure; the continuous line corresponds to $\Delta V/V_0(P)$ for Sm^{3+}]. Special technological measures[109] make it possible to prepare films of the metal modifica- tion of SmS stable at atmospheric pressure and with a lattice constant of 5.63 Å, which is very close to the value of a for the hypothetical phase $Sm^{3+}S$. [10]

The greatest theoretical interest lies in the metal phase of samarium monosulfide with the lattice con- stant 5.7 Å, which exhibits the fractional (interme- diate) valence of the Sm ion.

There are two possible ways of approaching the frac- tional valence of the Sm ion in SmS.

Variant A. The metal modification of samarium monosulfide is a mixture of Sm ions in the Sm^{2+} and Sm^{3+} states, which are distributed randomly throughout the lattice, and there are no changes from one state to the other (this is the case analogous to Eu_3S_4, Fe_3O_4, and other materials[11]).

Variant B. The samarium ion has mixed configura- tion and the electron wave eigenfunction of SmS con- sists of the sum of the wave functions of the localized $4f^6$ electrons φ_f and of the wave functions of the mix- ture of the $4f^5$ states and the conduction electrons φ_{cond}: $\Psi_k = a_k\varphi_{cond} + b_k\varphi_f$. The probability of finding an electron in the conduction band states is $n = \sum_k |a_k|^2$, where the summation is carried out over all the oc-

cupied states and the probability of finding an electron in the f state is $1 - n$. If an external perturbation local- izes an electron in the f state, its lifetime in this state is governed by the width (Δ) of the f levels: $\tau_{fl} = h/\Delta$. The experiments in which the measurement time is $t_{meas} < \tau_{fl}$ may reveal the f electrons separately in the $4f^6$ and $4f^5$ states, whereas experiments carried out with $t_{meas} > \tau_{fl}$ may reveal electrons in the mixed state.

The experimental data on the lattice constants simply indicate that the average valence of the Sm ions in Sms is fractional but they are insufficient to decide which of the above variants applies. This can only be done by analyzing the experimental data on the magnetic suscep- tibility and Mössbauer spectra.

2) *Magnetic susceptibility.* As pointed out above, the ground state of the Sm^{2+} ion ($^7F_0$) of the semicon- ductor phase $Sm^{2+}S$ is nonmagnetic ($J = 0$) and it cannot exhibit magnetic order at any temperature. The mag- netic properties of such Van Vleck ions are governed by the higher multiplet levels ($J > 0$). Their magnetic susceptibility χ should decrease with rising T (at high temperatures) because of the thermal filling of the multiplet and should be constant at low temperatures because, in this case, the thermal transfer is a weak effect and the "mixing" of the levels with $J = 0$ and $J = 1$ by an external magnetic field is the dominant fea- ture. (This contribution to χ is known as the Van Vleck temperature-independent magnetic susceptibil- ity.) The experimental data for χ of the semiconduc- tor phases of SmS, SmSe, and SmTe are in good agreement with this hypothesis[18,87,159,184] (curves 1, 2, and 3 in Fig. 13).[11]

If the semiconductor—metal phase transition occurs in accordance with the scheme $Sm^{2+} \to Sm^{3+} + e^-$, the presence of the trivalent samarium ions (ground state $^6H_{5/2}$, $J = 5/2$) may result in low-temperature magnetic ordering. However, the experimental results obtained down to ~ 0.4 °K show no sign of magnetic ordering and no contribution to χ of the component obeying the Curie law. The value of χ of the metal modification of SmS decreases, in the absolute sense, compared with the value for the semiconductor modification but remains independent of T below 100 °K, in contrast to other

---

[10] In the film variant it is possible to prepare SmS stable at atmospheric pressure and characterized by a range of lattice constants from 5.97 to 5.63 Å (beginning from $a = 5.7$ Å the metal modification is observed).[100,109,110]
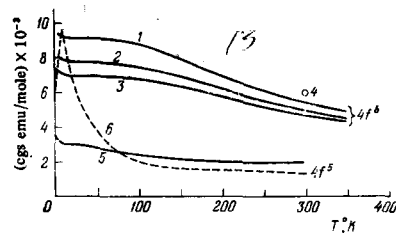
[11] The slight rise of χ at low temperatures is explained by the presence of a small amount of magnetic impurities in the in- vestigated samples.
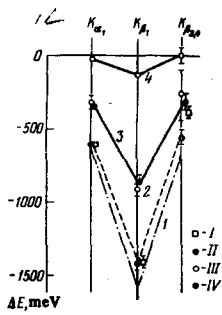
125   Sov. Phys. Usp. 21(2), Feb. 1978

I. A. Smirnov and V. S. Oskotskiĭ   125

FIG. 16. Dependences of δ and Γ on P applied to SmS. [186]

FIG. 14. Dependences of the x-ray shift on the type of line: 1) calculated dependences (see text); 2) calibration curves for SmF_3-SmCl_2 (I) and SmF_3—semiconductor phase of SmS (II) pairs; 3) metal phase of SmS at $P \gtrsim 9$ kbar (III) and $Sm_{0.8}Gd_{0.2}S$ (IV) at 300 °K; 4) low-temperature (77 °K) phase of $Sm_{0.8}Gd_{0.2}S$. All the experimental shifts are given relative to uncompressed SmS at 300 °K. [193]

compounds containing Sm^{3+} $(J = 5/2)$ [159,184] (compare curves 5 and 6 in Fig. 13). Varma and Yafet [76] demonstrated that, if the f shell of the samarium ion is in the mixed $4f^6-4f^5$ state, the susceptibility χ remains finite as the temperature approaches absolute zero. Thus, the data on the magnetic susceptibility support the variant B.

The fractional valence of the samarium ion in the high-pressure phase of SmS is supported by direct experimental evidence deduced from the Mössbauer spectra [185-188] and from the shifts of x-ray K lines. [189-196]

3) *Measurement of shifts of x-ray K lines.* It is demonstrated in [189,190] that the fractional valence of rare-earth compounds associated with the $4f$, $5d$, or $6s$ transitions can be investigated conveniently by the method of chemical shifts of x-ray K lines. This is due to a number of factors. [189,190,193]

a) The deep position of the $4f$ electrons in the atom is responsible for a large shift of the K lines (which is 10–20 times greater than the effects due to the $5d$, $6s$,
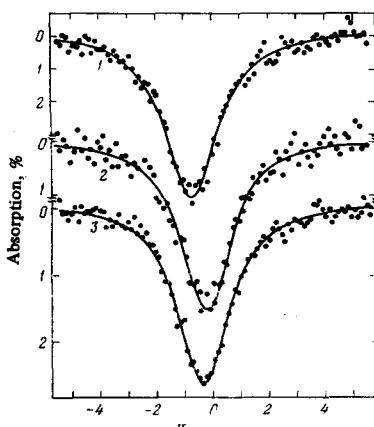
and p electrons) when an electron of this kind is removed or excited.

b) The dependence of the shift on the type of line then has the characteristic V shape for the $K_{\alpha_{1,2}}$, $K_{\beta_{1,3}}$, and $K_{\beta_{2,4}}$ lines (Fig. 14).

In investigations of the high-pressure phase of SmS the shift calibration curves (1 and 2 in Fig. 14) were found by Hartree–Fock–Slater calculations for $Sm^{3+}(4f^5)$ and $Sm^{2+}(4f^6)$ [197] and by the experimental determination of the relative shifts for the $Sm^{3+}F_3-Sm^{2+}Cl_2$ (curve 2 in Fig. 14, open squares) and $Sm^{3+}F_3-Sm^{2+}S$ (curve 2 in Fig. 14, black dots) pairs. The experimental curve 3 (Fig. 14, open circles) applies to the SmS–SmS pair, where the former is the high-pressure phase obtained at $P \gtrsim 9$ kbar and the latter is the semiconductor modification at atmospheric pressure. A comparison of the electron "facsimile" for the pairs 1, 2, and 3 in Fig. 14 shows that i) the valence of Sm in the high-ressure phase of SmS increases because of a reduction in the number of $4f$ electrons and ii) the number of $4f$ electrons removed from Sm is $\sim 0.62 + 0.03$ electrons/atom. This is close to the value obtained from the lattice constants (Table IV). Unfortunately, the small shift of the K line compared with its width makes it impossible to establish whether the K lines shifts as a whole or splits into two components, i.e., these data are insufficient to be able to decide between the variants A and B proposed for the description of the fractional valence of the samarium ion.

4) *Investigations of Mössbauer spectra.* Investigations of the dependence of the Mössbauer absorption (Fig. 15), isomeric shift δ, and line width Γ (Fig. 16) on hydrostatic pressure are reported in Refs. 29, 185–188. The isomeric shift δ has a discontinuity in the region of the phase transition. Throughout the investigated range of pressures (0–12 kbar), there is only one absorption line. This supports the hypothesis that our crystals contain indistinguishable samarium ions (variant B). This conclusion is also in agreement with the observation that the absolute value of Γ is the same before and after the phase transition. [12] Thus,

FIG. 15. Mössbauer spectra $(T = 300$ °K): 1) SmS at atmospheric pressure; 2) SmS at 11 kbar; 3) $Sm_{0.77}Y_{0.23}S$ at atmospheric pressure [185,186] (v is in units of mm/sec).
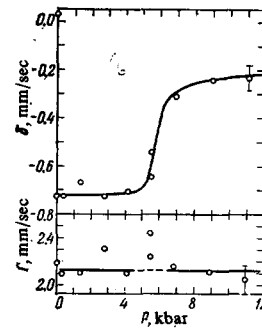
---

[12] The scatter of the values of $\Gamma(P)$ in the region of 6.5 kbar is an instrumental effect: the pressure is inhomogeneous at this point and this produces two (low- and high-pressure) phases in SmS. [186]
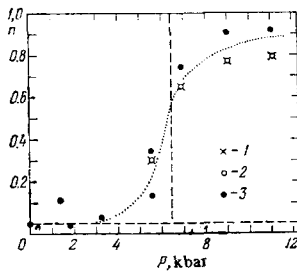
FIG. 17. Dependences $n = f(T)$ for SmS.[186] The various points represent an analysis of the data on δ on the assumption of the presence of delocalized d electrons in an incompressible (1) and a compressible (2) lattice, and on the assumption of localized electrons in an incompressible lattice (3).

FIG. 18. Dependences $\rho(T)$ (a) and $R_H(T)$ (b) for metal films of SmS with different lattice constants: 1) $a = 5.7$ Å; 2) 5.63 Å.[102] Here, R_H is in units of cm^3/C.

the experimental evidence is that the variant B applies to the high-pressure phase of SmS.

The data on δ can be used to determine n from Fig. 17[13] (the absolute value of n depends strongly on the model used in the calculations) and $\Delta\Gamma$ can be used to estimate the time associated with configuration fluctuations. This time is found to be $\tau_{f1} \lesssim 10^{-9}$ sec. It is interesting to note that SmS exhibits a considerable volume change in the pressure range 0–6.5 kbar (see Fig. 6). This may be due to the fact that a proportion of the "large" Sm^{2+} ions is transformed into the "small" Sm^{3+} ions before the phase transition. However, it is clear from Fig. 17 that $n \approx 0$ right up to $\sim P_{cr}/2$.

Table IV summarizes the values of the fractional valence of the Sm ion in the metal modification of SmS ($a \approx 5.7$ Å) obtained from various experiments.[14]

5) *Data on transport phenomena and electron component of the specific heat.* Information on the energy band structure of the metal modification can be obtained from an analysis of the experimental data on the transport phenomena and electron component of the specific heat C_e[85,102] (Figs. 18a and 18b). We shall now note certain special features of the behavior of the dependences $\rho(T)$, $R_H(T)$[102,15] and $C_e(T)$.[85]

a) The semiconductor film ($a = 5.97$ Å) exhibits the usual rise in ρ and R_H in the temperature range 1.5–300 °K.

b) The metal film 1 with $\alpha = 5.7$ Å (Fig. 18a) exhibits a temperature dependence $\rho(T)$ which can be divided

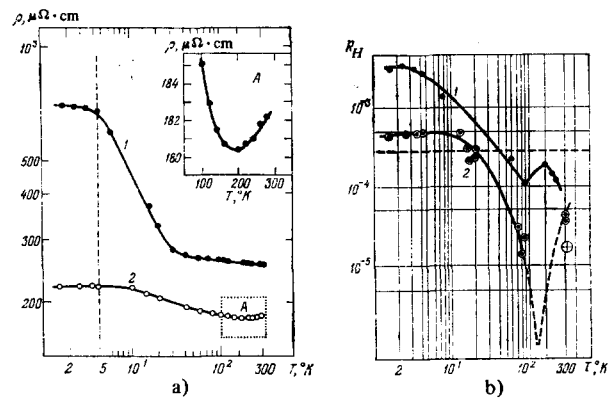[13]The calibration points in estimating n are the experimental values of δ of the semiconductor phase of SmS ($4f^6$ configuration, $\delta = -0.72 \pm 0.04$ mm/sec) and of Sm_2S_3 ($4f^5$ configuration, $\delta = -0.03 \pm 0.04$ mm/sec).

[14]Over twenty metals are not known to exhibit fractional valence of the rare-earth ion (these are the high-pressure phases of SmS, SmSe, SmTe, and Ce and the following compounds existing under normal conditions: SmB_6, $CePd_2$, $CeSn_3$, $CeAl_3$, $YbAl_2$, Th_xCe_{1-x}, $EuCu_2Si_2$, etc.[75]). This class of compounds is known in the literature as mixed-valence compounds or mixed-configuration compounds; they are sometimes called fluctuating-valence compounds or fluctuating-configuration compounds.

[15]The measurements of $\rho(T)$ and $R_H(T)$ were carried out on thin films.[102]

into three regions: the first extends from 1.5 to 4–5 °K and the second occupies the range 30–300 °K. In both these regions, the value of ρ is almost constant. These regions are separated by a third (intermediate) region where the resistivity varies.

c) The metal film 2 ($a = 5.63$ Å) exhibits the same behavior but the difference between the two plateaus of $\rho(T)$ is now much smaller and, moreover, beginning from 200 °K, the resistivity ρ rises with increasing temperature (Fig. 18a).

d) The behavior of the Hall coefficient R_H of these two metal films is unusual. A calculation of the carrier density on the assumption that each samarium atom gives up one electron to the conduction band ($N_0 = 4/a^3$) yields $N_0 \approx 2.2 \times 10^{22}$ cm^{-3} for these films. At temperatures above 20 °K (film 2) and above 40 °K (film 1), we have $N_H > N_0$, where N_H is the Hall carrier density calculated from $N_H = 1/R_H e$. (The dashed line 3 in Fig. 18b divides the regions so that, above this line, N_H deduced from R_H is $< N_0$ and, below the line, it is $> N_0$.)

e) At high temperatures, the film 2 exhibits a change in the sign of R_H from negative to positive (Fig. 18b).

f) The metal phase of SmS ($a = 5.7$ Å) is characterized by an anomalously high value of C_e, compared with the semiconductor modification.[85] At low temperatures, the total specific heat C_{tot} can be represented as the sum of C_e and of the lattice component C_l: $C_{tot} = C_e + C_l = \gamma_0 T + bT^3$, where γ_0 and b are constants which can be determined graphically from the dependence $C_{tot}/T = f(T^2)$ and γ_0 is a function of the density of states of free electrons at the Fermi level. The

TABLE IV.

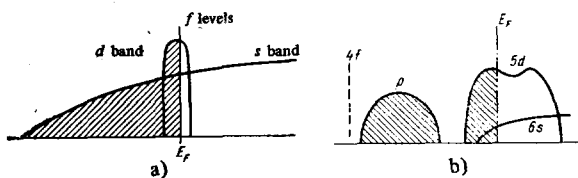| Experimental method	Valence of Sm ion
Lattice constant	2.77 ± 0.06
Shift of x-ray K lines	2.62 ± 0.03
Mössbauer effect	~ 2.8

FIG. 19. a) Energy band scheme of the metal modification of SmS.[102] b) Energy band scheme of $Ln^{3+}S$ metals.[83]

high-pressure phase of SmS has an anomalously large value of γ_0: ~145 mJ · mole^{-1} · deg^{-2} (for example, in, the case of Cu, its value is 0.69 mJ · mole^{-1} · deg^{-2} [82,140]).

There is as yet no generally accepted energy band structure of the metal phase capable of explaining these properties. An attempt to account for the properties of the metal phase on the basis of the following band scheme (Fig. 19a) is made in one of our earlier papers.[102] A wide s conduction band (formed from the $4f^6 6s$ states) is intersected by a narrow d band (originating from the $4f^5 5d$ states). The $4f^6$ levels coincide with the Fermi energy and lie inside the d band. The coincidence of the energies of the $4f^6$ and $4f^5 5d$ states is deduced from the experimental data on the absorption of light in the metal films of SmS[113,179]; a considerable reduction in the energy width of the d band in the metal compared with the semiconductor is observed.[113] Therefore, it is assumed in our paper[102] that the d band is narrow and the d electrons are localized near the ions.

The charge may be carried by the s or d electrons. Since an electron takes only 10^{-15} sec to pass a single samarium ion, i.e., this time is comparable with or shorter than τ_{f1}, such an electron "sees" the f shell of the samarium ion in the form of the separate states $4f^6$ and $4f^5$, which means that it "notices" fluctuations of the electron density charge and is scattered by them. This scattering is independent of temperature [Fig. 18a shows plateaus of $\rho(T)$ at 1.5-5 and 30-300 °K].

The abrupt fall in ρ in the temperature range 5-30 °K is explained by the influence of the d electrons. A d electron can reach a neighboring samarium ion only after overcoming a potential barrier of height of the order of 20 °K. At temperatures much below 20 °K, the jumps of the d electrons from ion to ion are of the tunnel type; they make a small contribution to the electrical conductivity, which is governed by the s electrons in this temperature range and is independent of temperature. At temperatures above ~20 °K, the barrier is no longer a hindrance and the motion of the d electrons is of the usual band nature. These electrons begin to make a considerable contribution to the electrical conductivity. Therefore, at $T > 20$ °K, the electrical resistivity decreases. This explains the fall in $\rho(T)$ in the range 5-30 °K and its independence of T above and below these temperatures.

The proposed model also explains the temperature dependence of R_H. At low temperatures, the d-electron mobility is much lower than the s-electron mobil-

ity. Thus, the contribution of the d electrons to the Hall effect is negligible and N_H represents only the s electrons. At high temperatures, the mobilities of the s and d electrons become comparable and R_H should then be discussed within the framework of the two-band model.

The energy band scheme (Fig. 19a) also explains the difference between the dependences $\rho(T)$ exhibited by the metal films with $a = 5.7$ and 5.63 Å. In the latter case, the number of electrons in the $4f^6$ states is small but there are also s and d electrons and the number in the last two categories is high than in SmS with $a = 5.7$ Å. Therefore, at low temperature, the conduction mechanisms are the same in both samples. At high temperatures, the smaller contribution of the "defects" (charge density fluctuations) in the film with $a = 5.63$ Å may result in the usual metallic nature of the electron scattering competing with the defect mechanism. This may account for the observed rise in $\rho(T)$ above 200 °K.

The band model of Fig. 19a also accounts for the high absolute value of γ_0 associated with the high density of states at the Fermi level. However, this band scheme is characterized by some indeterminacy due to the absence of direct experimental data (only indirect evidence is available[102]) on the position of the s band on the energy scale.

We shall conclude this section by noting that the energy band structure of the metal modification of SmS differs basically from the energy band structures of metallic trivalent rare-earth monosulfides[83] (Fig. 19b).

5. SOLID SOLUTIONS BASED ON SmS

An enormous amount of experimental data on solid solutions based on SmS is now available.[17-19,81-84,113,116,119,124-156,185-188,193-195,198-208] We cannot analyze these data in detail in the present review. We shall consider only the experimental data for the $Sm_{1-x}Gd_xS$ and $Sm_{1-x}Y_xS$ systems, which are typical representatives of the class of materials under discussion. We shall consider the available results in the next three subsections. In the first subsection we shall deal with the data on the phase transitions, in the second we shall discuss the experiments confirming the fractional valence of the samarium ions, and in the third we shall consider the papers whose analysis gives us information on the energy band structure of these materials.

A. Semiconductor–metal and metal–semiconductor phase transitions

The transition to the metal modification in all the solid solutions based on SmS occurs at a certain critical concentration of the dopant (impurity) x_{cr} (Figs. 20 and 21). The values of x_{cr} for $Sm_{1-x}Gd_xS$ and $Sm_{1-x}Y_xS$ are 0.15 and 0.16, respectively. The crystal lattice parameter first decreases continuously with rising x and then, on attaining the critical concentration, it falls rapidly to ~5.7-5.68 Å. At the point x_{cr} the color of the material changes from black to golden-yellow and usually many physical properties (transport coefficients, magnetic susceptibility, $\mathscr{R}$, etc.)
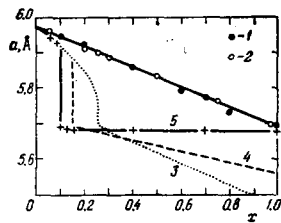
FIG. 20. Dependences of a on x for various $Sm_{1-x}M_xS$ solid solutions.[203] M^{2+}: 1) Ca, 2) Yb; M^{3+}: 3) Y, 4) Gd; M^{4+}: 5) Th.

FIG. 21. Dependence of the lattice constant on x for the $Sm_{1-x}Gd_xS$ solid-solution system.[81,124]

FIG. 22. Dependence of P_{cr} on x for the $Sm_{1-x}Gd_xS$ system.[81,124]

change abruptly. However, the type of the structure (NaCl) is retained. The necessary but not sufficient condition for the phase transition (known as chemical collapse) in such solid solutions is the presence in the lattice of a large, compared with sulfur (for example, As), or small, compared with Sm (Gd, Y, Th, etc.), dopant ion which acts as the "internal press." As pointed out at the beginning of this review, the compound used as a dopant should have a conduction band similar to that of SmS. [82,203] 16)

An important condition for chemical collapse is also a sufficiently high carrier density in the conduction band (see the discussion of the energy band structure given later).

The replacement of Sm and Ln^{3+} reduces the critical external hydrostatic pressure P_{cr} at which the substance goes over to the metal state. The internal lattice pressure rises from zero of $x = 0$ to 6.5 kbar for x_{cr}. By way of example, we shall consider the $Sm_{1-x}Gd_xS$ (Fig. 22) system. [81] When the pressure is removed, a sample with $x = 0.1$ returns to its initial form, whereas samples with $x = 0.13$, 0.14, and 0.15 retain the golden-yellow color right down to atmospheric pressure. [81,193] 17) They return to the initial form only after suitable annealing (Table V). [81] In the metal "golden" phase the $Sm_{1-x}Ln_x^{3+}S$ solutions exhibit, in a limited range of compositions $x_{cr} \leqslant x \leqslant x_{11m}$ (0.16 $\leqslant x$ $\lesssim 0.27$ for $Sm_{1-x}Gd_xS$, shown shaded in Fig. 21, and $0.15 \leqslant x \lesssim 0.3-0.4$ for $Sm_{1-x}Y_xS$), the following isostructural (NaCl-NaCl) metal-semiconductor (or metal-semimetal) transitions: a) a sudden transition as a result of cooling to 80-200 °K; b) a gradual transition as a result of heating to 600-900 °K.

The color of the material then changes from golden-yellow to black (the plasma minimum in Fig. 23 shifts toward lower energies with decreasing temperature), the lattice constant increases (Fig. 24), and there are abrupt changes in many physical properties. In some solid solutions the low-temperature phase transition is accompanied by an "explosion" which fractures a crystal or pulverizes it. 18) The phase transitions are re-

TABLE V.

Composition	Temperature of transition from "golden" to "black" phase, °C
$Sm_{0.87}Gd_{0.13}S$	140
$Sm_{0.86}Gd_{0.14}S$	220
$Sm_{0.85}Gd_{0.15}S$	350
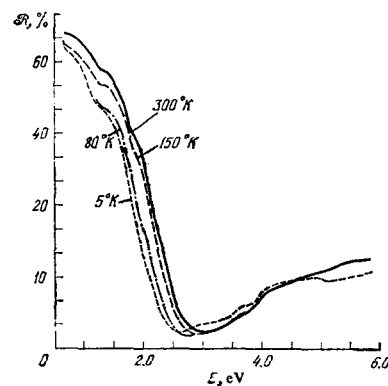
FIG. 23. Dependences of the reflection coefficient of $Sm_{0.72}Y_{0.28}S$ on the photon energy at various temperatures. [83]

16)Chemical collapse does not occur in the $Sm_{1-x}Ca_xS$ and $Sm_{1-x}Yb_xS$ systems[203] (Fig. 20), although it is expected on the basis of the lattice constants of CaS and YbS.

17)It is possible that, as in the high-pressure phase of SmS, there is a hysteresis of ~4 kbar, but since these compositions are characterized by $P_{cr} < 4$ kbar, the "golden" phase is retained at atmospheric pressure.

18)The metastable metal modification of $Sm_{1-x}Gd_xS$, obtained under hydrostatic compression of samples with $x = 0.13-0.15$ also exhibits the "explosive" low-temperature phase transition.

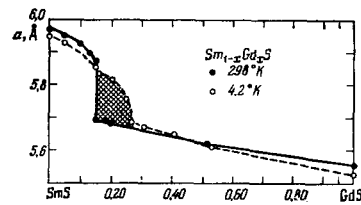FIG. 24. Dependence $a(T)$ for $Sm_{0.83}Gd_{0.17}S$. [81,124]

I. A. Smirnov and V. S. Oskotskiĭ
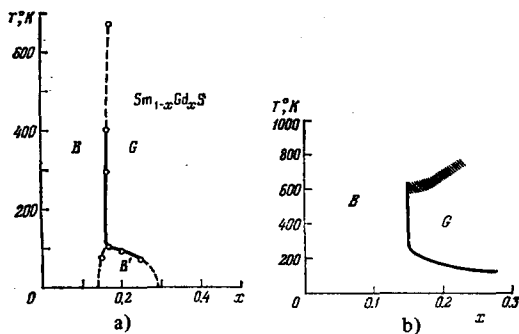
FIG. 25. Temperature–x phase diagrams of $Sm_{1-x}Gd_xS$[81] (a) and $Sm_{1-x}Y_xS$[146] (b). Here, B denotes the "black" phase and G the "golden" phase.

versible. When T is increased, in the case of the low-temperature transition, or when it is lowered, in the case of the high-temperature transition, the initially black crystals (or the resultant powder) again become golden-yellow. The low-temperature phase transition is characterized by a considerable hysteresis in the case of $Sm_{1-x}Gd_xS$[81,152]; this hysteresis is not exhibited by some $Sm_{1-x}Y_xS$ solid solutions ($x = 0.19$ or 0.23).[146] The compositions close to x_{cr} (on the "golden" phase side) have a number of special properties.[146] Figure 25 shows the T–x phase diagrams for two of the solid solutions considered (B and G are the regions where the "black" and "golden" phases exist).[81,146]

B. Metal modification. Experimental data confirming fractional valence of the Sm ion

The valence state of the Sm ion in solid solutions can be determined by the same methods as those employed for SmS (investigations of the lattice constants and Mössbauer spectra, determination of the shifts of x-ray K lines, study of the magnetic susceptibility). Two additional methods have been used for this purpose: these involve determination of the x-ray[199–204,205–206] and ultraviolet[205] photoelectron spectra.

1) *Crystal lattice constant and* $\Delta V/V_0 = f(x)$. The valence state of the Sm ions in $Sm_{1-x}Ln_x^{3+}S$ solid solutions can be determined by linear interpolation between the experimental dependences $a(x)$ and the calculated theoretical lines $e(x)$, corresponding to the 2+ and 3+ valences of the Sm ion[82] (Fig. 26); the expression for $e(x)$ includes a_0, which is the lattice constant of SmS. This method makes it possible to estimate the order of magnitude of the valence of Sm (see Fig. 30 below, data for the $Sm_{1-x}Y_xS$ system). Similar values are also obtained for $Sm_{1-x}Gd_xS$.
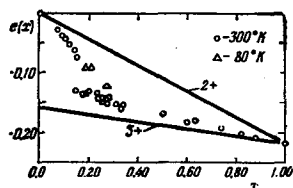

FIG. 26. Dependences $e(x)$ for $Sm_{1-x}Y_xS$.[82]
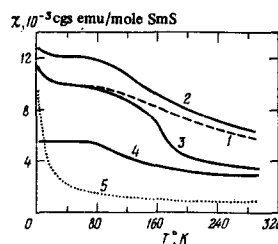

FIG. 27. Temperature dependence of χ for the $Sm_{1-x}Y_xS$ system[146]: 1) $x = 0$; 2) $x = 0.12$; 3) $x = 0.23$; 4) $x = 0.88$; 5) Pd_3Sm with Sm^{3+}.

2) *Magnetic susceptibility*. Comparison of the temperature dependences of the susceptibility $\chi(T)$ for solid solutions and SmS can be carried out using $Sm_{1-x}Y_xS$, because the Y ions are nonmagnetic. The dependence of χ on T for the high-pressure phase of SmS is completely identical with that for the chemically collapsed "golden" modification of $Sm_{1-x}Y_xS$ (compare Figs. 13 and 27),[146] which shows that the Sm ions in these phases are in the same (or similar) valence states.

3) *Measurements of shifts of x-ray K lines*. Figure 14 (curve 3) gives the shifts of the x-ray K lines for the chemically collapsed metal phase of $Sm_{0.8}Gd_{0.2}S$.[193] We can see that the effective valence of Sm in this phase is equal to its valence in the high-pressure phase of SmS and it amounts to 2.63 ± 0.03.[19] The same figure shows the data for the "black" phase of $Sm_{0.82}Gd_{0.18}S$, obtained as a result of the low-temperature phase transition (produced by cooling the sample to $77\,°K$). The valence of the Sm ions in this phase is 2.08 ± 0.01. Egorov *et al.*[195] were the first to show convincingly that the valence of the Gd ion in $Sm_{1-x}Gd_xS$ solid solutions (and that of Nd in the $Sm_{1-x}Nd_xS$ system) remains constant within the limits of experimental error (Fig. 28).[20]

4) *Investigations of Mössbauer spectra*. The close similarity of the metal modification of SmS and the phase obtained by chemical collapse in $Sm_{1-x}Y_xS$ is observed also in studies of the Mössbauer spectra[186] (see Fig. 15): there is one maximum in the absorption curve, the limiting value of τ_{t1} is the same, the effective valence of the Sm ions is similar, etc. As in the case of the metal phase of SmS, the data deduced from the Mössbauer spectra (and magnetic susceptibility) of the collapsed phase of $Sm_{1-x}Y_xS$ indicate the presence of Sm ions of mixed valence.

5) *Investigations of x-ray photoelectron spectra*. The essence of this method is to illuminate a solid with photons of energy amounting to a few keV and to find the energy distribution to the emitted electrons.[75] By way of example, Fig. 29 shows the data for the metal

---

[19] The same method was used by Grushko *et al.*[194] to determine the effective valence of the Sm ions in $Sm_{0.8}Nd_{0.2}S$. This valence found to be 2.64 ± 0.03.

[20] An interesting feature of the dependence $\rho(x)$ is exhibited by the $Sm_{1-x}Gd_xS$ system[195]: the fall of ρ ends well before the onset of the phase transition (Fig. 28). It is suggested[195] that the presence of a conducting impurity (in this case Gd) in a sufficiently high concentration may result in a strong reduction in ρ because of the "percolation" effect.
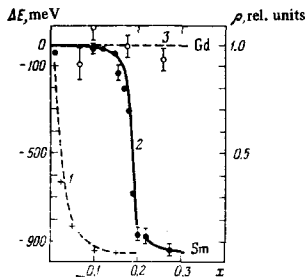
FIG. 28. Shift of the K_{β_1} lines of Sm (2) and Gd (3), and values of ρ (1) plotted as a function of x for the $Sm_{1-x}Gd_xS$ system. [195]

FIG. 30. Effective valence of the Sm ions in $Sm_{1-x}Y_xS$ [82] deduced from various experiments: 1), 2) from lattice constants at temperatures of 293 and 80 °K, respectively; 3) from Mössbauer spectra; 4), 5) from x-ray photoelectron spectra obtained at 293 and 110 °K.

phase with $Sm_{0.81}Y_{0.19}S$ composition. [207] The comparison standards are the crystals of YS (without the $4f$ electrons), SmS (semiconductor modification with Sm^{2+}), and SmAs (with Sm^{3+}). We can see from Fig. 29 that the spectra of $Sm_{0.81}Y_{0.19}S$ include peaks corresponding to Sm^{2+} and Sm^{3+}. Cooling reduces the ratio Sm^{3+}/Sm^{2+}. The determination of the proportions of Sm^{3+} and Sm^{2+} in this solid solution is complicated by the need to allow correctly for the relatively strong background (see Fig. 29). It is necessary also to postulate that the surface properties (which are investigated in this experiment) are identical with those of the bulk of the crystal. The results of calculations of the effective valence of the Sm ions in $Sm_{1-x}Y_xS$ are plotted in Fig. 30. The recorded spectra have well-resolved peaks corresponding to the $4f^6$ and $4f^5$ configurations of the Sm ion. Since the measurement time in such experiments is $\sim 10^{-16}$ sec, it follows—in conjunction with the Mössbauer spectra—that τ_{f1} lies within the range 10^{-9}–10^{-16} sec.

6) *Investigations of mechanical properties.* The bulk modulus B, defined by $B = (C_{11} + 2C_{12})/3$, of $Sm_{1-x}Y_xS$ solid solutions has been determined. [141,143] At x_{cr} we find that $B \to 0$. The "softness" of metal phase (corresponding to $x \geq x_{cr}$) indicates mixed valence of the Sm ions in these solutions. [143]
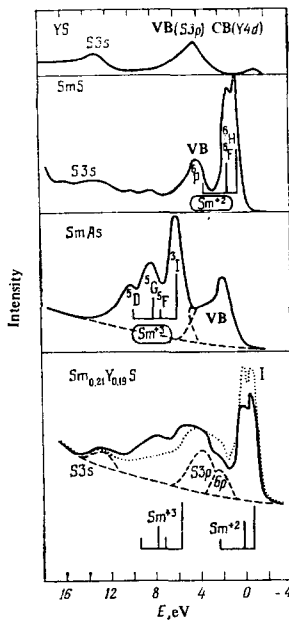
FIG. 29. X-ray photoelectron spectra of YS and SmS (semiconductor phase, Sm^{2+}), SmAs (with Sm^{3+}), and $Sm_{0.81}Y_{0.19}S$ at 296 °K (continuous curves). Curve I represents the results obtained at 110 °K. [207] Here, VB is the valence band and CB is the conduction band.
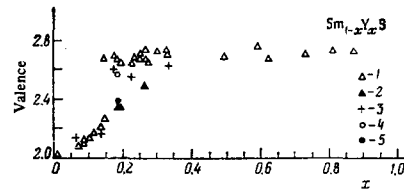
7) *Investigations of Raman scattering spectra.* Unusual results are obtained from the Raman scattering spectra of the metal phase of $Sm_{1-x}Y_xS$ ($0 \leq x \leq 0.4$). It is found that the results for the compositions with $x < x_{cr}$ and $x > x_{cr}$ can be explained by transitions occurring only inside the ^7F_J multiplets typical of the $4f^6$ configuration of Sm^{2+}, i.e., there is no Raman scattering for Sm^{3+}. [144,148] Figure 31 shows, by way of example, the experimental data for the "golden" ($T = 300$ °K) and "black" ($T = 77$ and 2 °K) phases of $Sm_{0.77}Y_{0.23}S$. The latter phase is produced by the low-temperature transition. It is clear from Fig. 31 that the transition from the "golden" to the "black" modification does not alter the Raman scattering spectra.

C. Characteristics of the energy band structure

In the early studies of the $Sm_{1-x}Ln_x^{3+}S$ solid solution system the metal modification ($x_{cr} \leq x \leq x_{1m}$) has been identified completely with the high-pressure phase of Sms. However, more detailed investigations of these solid solutions have shown that its situation is slightly different. There are many indications that the two phases are identical: the temperature dependences of the magnetic susceptibility are the same (this applies to solid solutions with a nonmagnetic dopant), the lattice constants are the same, the effective valence of the Sm ions is similar, there are similarities in the optical properties and so on. However, the metal phase of the solid solutions contains "foreign" ions (Ln^{3+}, As, etc.) and, therefore, it has a number of special properties which distinguish it from the high-pressure phase of SmS. These properties are manifested in the transport phenomena, conduction band structure, existence of the low- and high-temperature phase transitions, Mössbauer spectra, etc. [75,83,119,142,186] Moreover, the mechanism of the phase transition under hydrostatic pressure (SmS) differs from that which occurs as a result of an increase in the dopant
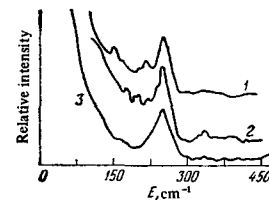
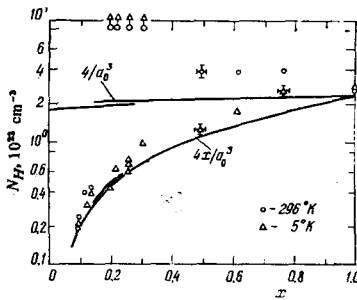FIG. 31. Raman scattering spectra[148]: 1) 300 °K ("golden" phase); 2), 3) 77 °K and 2 °K ("black" phase).

FIG. 32. Dependences of the Hall carrier density on the composition of $Sm_{1-x}Y_xS$. [82]

o − 296 °K
△ − 5 °K

FIG. 33. Schematic representation of the dependences of the density of states on the energy in $Sm_{1-x}Y_xS$. [82,140]

a) E_F, f, SmS, d

b) $Sm_{0.91}Y_{0.09}S$

c) $Sm_{0.67}Y_{0.33}S$

$N(E)$

E

$(Sm_{1-x}Ln_x^{3+}S)$; for details see below. The Ln^{3+} ions play an important role in the formation of the conduction band of $Sm_{1-x}Ln_x^{3+}S$. These ions a) act as electron sources and b) are mainly responsible for the reduction in the gap between the localized $4f$ levels and the bottom of the conduction band. [82,142] A model of the conduction band of $Sm_{1-x}Y_xS$ (typical of solid solutions based on SmS) has been constructed (subject to a number of approximations) on the basis of the experimental data relating to the transport phenomena[82,142] and then confirmed qualitatively by investigations of the optical properties,[83,133] electron component of the specific heat,[82,140] etc. We shall now consider how this model is constructed. The experimental values of the Hall coefficient R_H for the "black" phase ($x \leqslant 0.17$ at 300 °K and $\lesssim 0.4$ at 5 °K) and for compositions close to YS can be described using the one-band model (Fig. 32). Here, $N_H = 1/R_H e$ is the Hall carrier density deduced from the experimental results: $4/a^3$ is the carrier density deduced from the x-ray density of the crystal; $4x/a^3$ is the density of the Y electrons alone. A considerable deviation from the one-band model is observed in the range $0.17 \leqslant x \lesssim 0.4$. This behavior can be explained by a band model shown in Fig. 33[82,142] which allows for the dependence on x of the mutual positions of two subbands with low and high densities of states (f and d subbands).[21)]

The carrier density rises when Y is added ($Sm_{0.91}Y_{0.09}S$). Since the lattice constant decreases, the conduction band moves toward the f levels, which penetrate into the d band and, because of the $f–d$ interaction, expand into a narrow band. [75] Since the band is filled with d electrons of the Y atoms, E_F lies above f band. In this situation the Sm ion remains divalent and R_H represents only the electron density in the d band (see Fig. 32). The samples remain black since the plasma minimum is still located in the infrared (Fig. 34a). The variable valence of the ions is manifested by the compositions for which E_F intersects the f and d states ($Sm_{0.67}Y_{0.33}S$). Now, R_H can no longer be described by a simple band model. The samples become golden since an increase in the d-electron density shifts the plasma minimum to the visible part of the spectrum (Fig. 34b). At lower temperatures the

energy band structure of the compositions with $0.17 \leqslant x \lesssim 0.4$ assumes the form shown in Fig. 33b. In the case of YS there are no f levels and in the case of GdS they are located lower on the energy scale than the p band (Fig. 19b) and they do not participate in the formation of the conduction band so that R_H is described satisfactorily within the framework of the one-band model (see Fig. 32). It is somewhat more difficult to interpret the energy band structure on transition from the compositions with $x \geqslant 0.4$ to those with $x = 1$. The band structure of Fig. 33 is confirmed qualitatively by the experimental results on the reflection spectra, electrical conductivity, and low-temperature specific heat.

D. Analysis of reflection spectra and electrical conductivity

Information on the relative positions of the $4f$ levels and E_F can be obtained from the carrier scattering time τ_0 at zero frequency. The values of τ_0 can be calculated from the dc electrical conductivity σ and from the plasma frequency ω_p; they describe the scattering processes in the range $\pm kT$ near E_F[83,133] (Fig.

$R,\%$

a)

SmS
$Sm_{0.95}Y_{0.05}S$
$Sm_{0.86}Y_{0.14}S$
$Sm_{0.92}Y_{0.08}S$

b)

YS
$Sm_{0.67}Y_{0.33}S$
$Sm_{0.82}Y_{0.18}S$

E, eV
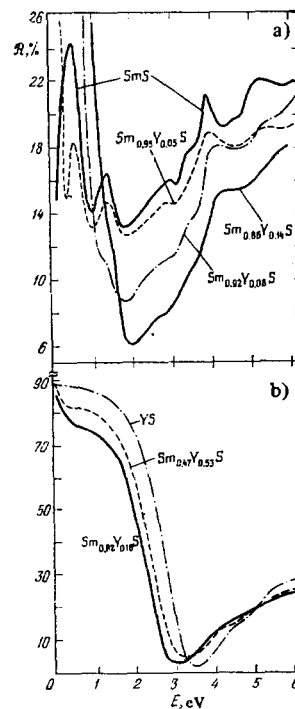
FIG. 34. Dependences of R of $Sm_{1-x}Y_xS$ on the photon energy[83]: a) "black" phase; b) "golden" phase.

[21)]For simplicity, it is assumed[82,142] that the system has one common d band and that the d electrons of the f^5d configuration of Sm are equivalent to those in the d band is ignored in this model.
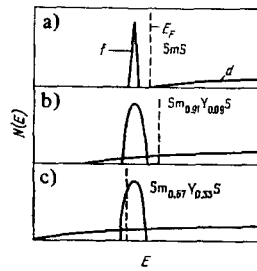
10^{-14}
τ_0, sec
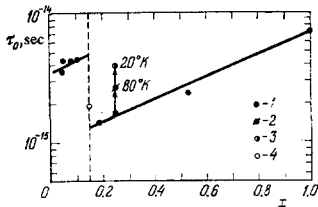$20°K$
$80°K$
10^{-15}

●-1
●-2
●-3
○-4

0   0.2   0.4   0.6   0.8   1.0
x

FIG. 35. Dependence of τ_0 on x for $Sm_{1-x}Y_xS$[83,134]: 1) 296 °K; 2) 80 °K; 3) 20 °K; 4) SmS (high-pressure phase).

35). For $x < x_{cr}$ ("black" phase) the value of τ_0 does not depend strongly on x (Fig. 33b) but it falls abruptly at the point x_{cr}. This is evidence of strong resonant scattering of the conduction electrons by E_F (Fig. 33c). For the composition with $x = 0.25$ the value of τ_0 rises on cooling to 4 °K, reaching a value typical of the "black" samples with $x < x_{cr}$ (see Fig. 33b): cooling produces the low-temperature phase transition. The linear rise of τ_0 on approach to YS is due to a reduction in the number of resonance states of Sm.

E. Data on the specific heat of $Sm_{1-x}Y_xS$ solid solutions

The data on the low-temperature specific heat[82,140] indicate a high value of γ_0 (Table VI) for the metal phase of $Sm_{1-x}Y_xS$ ($0.17 \leqslant x \leqslant 0.4$), which corresponds to a high density of states at the Fermi level. The value of γ_0 is small for the "black" phase ($0.17 \leqslant x$) and for YS. This is in satisfactory agreement with the energy band schemes in Figs. 33b and 33c.

We shall conclude the experimental part of our review by formulating the main requirements which the theory must satisfy.

The theory should:

1) give a description of the semiconductor—metal phase transition in SmX under hydrostatic pressure;

2) account for the sudden phase transition in SmS and the gradual one in SmSe and SmTe;

3) explain the phase transition in $Sm_{1-x}Ln_x^{3+}S$ at x_{cr};

4) explain the low- and high-temperature metal-semiconductor phase transitions in solid solutions based on SmS; and, finally,

5) explain the reason for the appearance of and justify theoretically the phenomenon of variable valence in the metal modification of SmS and in solid solutions based on it.

We shall attempt to fulfill some of these requirements in Sec. 6.

TABLE VI. Values of γ_0 for $Sm_{1-x}Y_xS$ solid-solution system. [124]

Composition	γ, mJ ·mole^{-1}·deg^{-2}	Composition	γ, mJ ·mole^{-1}·deg^{-2}
SmS	0±1	$Sm_{0.67}Y_{0.33}S$	50±5
$Sm_{0.91}Y_{0.09}S$	2±1	YS	4±1
$Sm_{0.77}Y_{0.23}S$	14±5		

6. REVIEW OF THE THEORIES OF THE PHASE TRANSITION IN SmS

The phase transition which occurs in SmS under a pressure of 6.5 kbar is characterized by a sudden increase in the number of the conduction electrons to a value typical of metals, i.e., to about one electron per samarium ion. All theories start from the assumption that an electron is transferred to the conduction band from the $4f^6$ shell when the energy of the $4f^6$ state becomes comparable, under the influence of pressure, with the energy at the bottom of a conduction band formed from the $4f^5$ + electron state in the $6s$, $5d$, or hybrid $6s5d$ state. Under normal pressure this energy gap should amount to a few hundredths of an electron-volt so that it can collapse at 6.5 kbar on the assumption that the deformation potential has its usual value of a few electron-volts.

Mott[82] suggested that in the presence of a gap the excited states are of the exciton rather than of charge-carrying nature, but when the band collapses and the exciton concentration rises these states overlap forming a conduction band.

The conduction band of the metal phase differs greatly from the conductor band of the semiconductor modification, formed from the $4f^6 6s$ states. Therefore, the energy gap between the f levels and the conduction band of the semiconductor is not equal to the gap which has to be overcome for the phase transition to occur.

Thus, compression produces a phase transition in SmS. We shall now consider why this transition is abrupt and why the number of conduction electrons per samarium ion in the final state is fractional (like the number of f electrons).

The fractional valence is not an exceptional phenomenon. The conduction band of many metals, particularly transition elements, overlaps other bands forming hybrid structures and an electron may belong simultaneously to two bands. The effective number of electrons in a given band per atom is then fractional. In the case of SmS and other rare-earth compounds the fractional valence means that the Sm ion has a fractional number of the localized f electrons. This does not apply if the f-electron energy is higher than the bottom of the conduction band. Then, some of the f electrons fill the states in the conduction band below the f level and the remainder are located at the f level, which coincides with the Fermi energy E_F. The interaction of the f electrons with the conduction-band electrons results in hybridization: the f-electron level broadens into a band in which the electron wave function φ consists of two terms $a\varphi_f + b\varphi_{cond}$ describing the localized state (φ_f) and the delocalized conducting state (φ_{cond}). In view of the localized nature of the f states the hybridization results in broadening by no more than 10^{-2}–10^{-1} eV, so that inside the conduction band there is a narrow band with a higher density of the electron states which are of localized nature. The Fermi level cannot be above this band because the total number of the f states is equal to the number of electrons; therefore, the Fermi level can be either inside this band or

below it. In the former case we have the fractional valence state. We shall now consider its stability.

In discussing the stability one has to analyze the energy of a crystal. Since the f shell is localized inside an ion, a change in the interionic distances in a crystal as a result of compression has little effect on its energy so that the forbidden band becomes narrower because of the dropping of the bottom of the conduction band. If n electrons are transferred to the conduction band, the energy is

$$E = \mathscr{E}_g n + An^{5/3}, \tag{1}$$

where $\mathscr{E}_g$ is the distance from the f level to the bottom of the conduction band; $An^{5/3}$ is the energy of the electrons with the Fermi distribution in the conduction band; n is the density of electrons in the conduction band per samarium ion

$$A = \frac{3^{5/3}\pi^{4/3}\hbar^2}{2^{5/3}5m^*a^2}; \tag{2}$$

m^* is the effective mass; a is the lattice constant of SmS. Clearly, if $\mathscr{E}_g > 0$, i.e., if the f levels lie below the bottom of the conduction band, E has a minimum at $n = 0$ and all the electrons are in the f levels. Compression reduces $\mathscr{E}_g$ to zero and then this energy becomes negative. The bottom of the conduction band drops below the f levels and E has a minimum at $n > 0$ so that further compression results in a smooth rise of n to unity. This corresponds to a gradual phase transition.

The abrupt phase transition may be explained by supplementing the energy (1) with "acceleration" terms, i.e., those which reduce the energy with rising n at a rate faster than the rise of the energy due to the term $An^{5/3}$. Falicov, Kimball, and Ramirez[209,210] suggested allowance for the mutual Coulomb attraction of the conduction electrons and holes remaining in the f shells, which contributes the energy term $-Bn^2$. Therefore, in their model

$$E = \mathscr{E}_g n + An^{5/3} - Bn^2. \tag{3}$$

When the quantity $\mathscr{E}_g$ becomes negative, this function has two extrema: a minimum at a lower value of n and a maximum at a higher value, which corresponds to a gradual phase transition. However, further compression brings the two extrema closer, so that they eventually form an inflection point and the function $E(n)$ becomes monotonically decreasing, since the stable state is reached at $n = 1$. This occurs when

$$\frac{dE}{dn} = \mathscr{E}_g + \frac{5}{3} An^{2/3} - 2Bn = 0,$$
$$\frac{d^2E}{dn^2} = \frac{10}{9} An^{-1/3} - 2B = 0. \tag{4}$$

The value of $\mathscr{E}_g$ is then

$$\mathscr{E}_g = -\sqrt[3]{\frac{5AB^2}{9}}$$

and

$$n = \left(\frac{5A}{9B}\right)^3.$$

This model describes an abrupt phase transition, but it cannot account for the fractional valence after the phase transition.

So far we have ignored the elasticity of the lattice assuming it to be incompressible. However, the considerable change at the phase transition point shows clearly that the lattice compressibility cannot be ignored and the stability condition should be regarded as the requirement for a positive compressibility:

$$\beta = -\frac{1}{V}\frac{dV}{dP} = \frac{1}{V}\left(\frac{d^2E}{dV^2}\right)^{-1} > 0,$$
$$(\beta > 0, \text{ i.e., } d^2E/dV^2 > 0), \tag{5}$$

where V is the volume and P is the pressure. This approach is developed in a number of papers.[24,45,51,77] Hirst[45] ignored the term suggested by Falicov, Kimball, and Ramirez indicating that the electron–hole interaction in the metal phase of SmS may be strongly weakened by the screening effect of the conduction electrons. This approach was followed by Jefferson,[51] who strengthened Hirst's arguments by pointing out that the matrix element of the Coulomb interaction between the f and d (or s) electron states should vanish because of the opposite parity of the corresponding wave functions and because of the centrally symmetric position of the Sm ion in the SmS lattice. The energy should include explicity the terms depending on the lattice volume. We shall assume that $\mathscr{E}_g$ is a linear function of the volume V and we shall take the initial volume V_0 to be the one for which $\mathscr{E}_g = 0$. Then, $\mathscr{E}_g = \alpha_0 \Delta V$, where $\Delta V = V - V_0$. We shall include the elastic terms up to the third order in ΔV, bearing in mind that the anharmonicity can make a considerable contribution to the energy in the case of the strong deformation which accompanies the phase transition. The energy becomes

$$E = \alpha_0 \Delta V n + An^{5/3} + B\Delta V + \frac{D}{2}(\Delta V)^2 - \frac{1}{6}F(\Delta V)^3. \tag{6}$$

The term linear in ΔV occurs because V_0 is the nonequilibrium volume and the negative sign of the term cubic in ΔV ensures an increase in the stiffness resulting from compression. For a given volume, the value of n is found by minimizing the energy

$$\frac{\partial E}{\partial n} = 0 = \alpha_0 \Delta V + \frac{5}{3} An^{2/3}, \tag{7}$$

and then we find n as a function of ΔV. If $V > V_0$, we have $n = 0$, $d^2E/dV^2 = D - F\Delta V$ and $\beta = 1/V(D - F\Delta V)$ is the usual compressibility of the crystal lattice (section ab in Fig. 36). If $\Delta V < 0$, then

$$\frac{d^2E}{dV^2} = \frac{d^2E}{d(\Delta V)^2} = \frac{\partial^2E}{\partial \Delta V^2} + \frac{\partial^2E}{\partial \Delta V \partial n}\frac{dn}{d\Delta V}$$
$$= D - F\Delta V - \frac{3}{2}\alpha_0^{5/2}\left(\frac{3}{5A}\right)^{3/2}|\Delta V|^{1/2}. \tag{8}$$

We can see that an increase in $|\Delta V|$ causes $d^2E/d(\Delta V)^2$ initially to decrease because of the increase in the energy resulting from the transfer of electrons to the conduction band (section bc in Fig. 36) so that it may fall to zero and become negative. The compressibility then also becomes negative, i.e., the volume of the crystal may decrease as a result of a reduction in
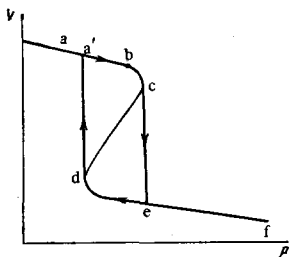
FIG. 36. Schematic dependence of the volume V on the pressure P in the course of the phase transition in SmS.

pressure (section cd in Fig. 36). The second term in d^2E/dV^2 then makes an increasing positive contribution which can again make d^2E/dV^2 positive. The compressibility returns to positive values (section df in Fig. 36). The abrupt phase transition occurs along the ce line in Fig. 36. If $n < 1$ at the point e, the valence after the phase transition is fractional and a further compression causes n to rise gradually approaching unity. When the applied pressure is reduced, the state of the crystal follows the curve fda'a, i.e., hysteresis is exhibited: the metal phase exists at pressures lower than the pressure corresponding to the semiconductor−metal transition.

Likely parameters of this model can be selected but one can hardly expect the same values for the semiconductor and metal phases.

The theory of the phase transition in the mixed compounds of the $Sm_{1-x}Ln_x^{3+}S$ type can be developed in a similar manner. [51,63] An allowance is made for the influence of the impurity on the initial volume of a crystal (chemical compression), which alters the gap from the f levels to the bottom of the conduction band in the metal phase; the influence on the density of electrons in the conduction band is also allowed for.

The published treatments have ignored so far the hybridization between the f states and those in the conduction band. However, it has been shown[58,59] that allowance for this hybridization may lead to a prediction of a phase transition and of a stable state with fractional valence. Since the wave functions of atomic origin in a crystal are no longer the eigenfunctions of the Hamiltonian because of the additional interactions, this Hamiltonian should include not only the diagonal terms but also the cross terms between the various states. Khomskiĭ and Kocharyan[58,59] allowed for the usual cross terms between the f and conduction-band states, and also for the terms representing the Coulomb interaction between them. The Hamiltonian then becomes

$$\mathscr{H} = \sum_i E_0 b_i^+ b_i + \sum_k \varepsilon_k a_k^+ a_k + \frac{V}{N} \sum_{k,i} (a_k^+ b_i + \text{H.c.}) + \frac{g}{N} \sum_{kk'i} a_k^+ a_{k'} b_i^+ b_i;$$

(9)

here, the first term is the energy of the localized f states, the second is the energy of the conduction electrons, the third describes the hybridization, and the fourth represents the energy of the repulsion between the localized f electrons and the conduction electrons. They demonstrated that the second and third terms broadened the f energy states and this broadening is

particularly strong when the f levels are inside the conduction band near the Fermi energy. Estimates indicate that solely because of the Coulomb interactions this broadening may reach 0.04−0.1 eV. In this model the compression of a crystal reduces the gap between the f levels and the bottom of the conduction band; then, the f electrons penetrate the conduction band and the Falicov-type direct Coulomb interaction between the localized and conduction electrons tends to increase n to unity in an abrupt manner. However, in the course of this transition the narrow f level is located near the Fermi energy and, therefore, it acquires a considerable width. This reduces the energy of the occupied f states (since the f states are now located not only at the Fermi level but also considerably lower). Nevertheless, an increase in the conduction electron density and a reduction in the number of the f electrons shift the Fermi level to the lower part of the broadened f-state band, so that the overall position of the energy of the occupied f states is lowered because of broadening (it should be noted that if the f states lie above E_F, this effect disappears completely). This may result in minimization of the energy in the $n < 1$ case, i.e., it may produce a stable phase with fractional valence.

The broadened f-state band near E_F is responsible for the increase in the density of states in this region, which may account for the large contribution of the conduction electrons to the specific heat. [65]

We can see that both approaches—allowance for the elastic forces and allowance for the hybridization—are capable of describing the main properties of the phase transition in SmS. Clearly, both factors contribute simultaneously to the observed effect. Kocharyan and Khomskiĭ[59] made an attempt to unify the two approaches. It is now evident that new experimental investigations are needed to estimate the contributions of the two factors.

7. CONCLUSIONS

We can see from this review that samarium monochalcogenides are extremely interesting objects to experimentalists and theoreticians. Many aspects of our knowledge of this class of materials are either controversial or still unclear. There is as yet no full picture of the pressure and temperature dependences of the electrical, magnetic, optical, and mechanical properties of samarium monosulfide in the semiconductor and metal phases. Further studies will help to determine in detail the electron structure and its change as a result of the phase transition, and to estimate the role of the various mechanisms in this transition.

The unique semiconductor−metal and metal−semiconductor phase transitions occurring in SmS and in solid solutions based on this compound are beginning to find practical applications. One of the examples is the use of the metal−semiconductor phase transition in thin SmS films for information recording and storage. [103 105,114] These films have been used in making amplitude-phase holograms with a recording energy of ~30 mJ/cm², diffraction efficiency ~3%, and reasonably high resolution (up to 2000 lines/mm). [103,114]

I. A. Smirnov and V. S. Oskotskiĭ   135

Even within the fairly unrestricted framework of the present review we have been unable to review in full detail the enormous amount of the experimental and theoretical data on SmS, SmSe, SmTe, and solid solutions based on SmS. We have decided to list almost all the known literature on SmS and its solid solutions. For a more detailed bibliography of the work done the reader is directed to the mongraph by Golubkov et al.[1] and to bibliographical collections published by the Ioffe Physicotechnical Institute of the USSR Academy of Sciences, together with the Library of the Academy.[211] The latter give a selection of work on SmTe and SmSe, which could not have been covered in the present review.

[1]A. V. Golubkov, E. V. Goncharova, V. P. Zhuze, G. M. Loginov, V. M. Sergeeva, and I. A. Smirnov, Fizicheskie svoǐstva khal'kogenidov RZÉ (Physical Properties of Rare-Earth Chalcogenides), Nauka, L., 1973.

[2]Yu. A. Firsov, in: Trudy zimneǐ shkoly po fizike poluprovodnikov (Proc. Winter School on the Physics of Semiconductors), Ioffe Physicotechnical Institute, Academy of Sciences of the USSR, L., 1971.

[3]S. Methfessel and D. C. Mattis, "Magnetic semiconductors," in: Handbuch der Physik (ed. by S. Flügge and H. P. J. Wijn), Vol. 18, Part 1, Springer Verlag, Berlin, 1968, pp. 389–562 (Russ. Transl. Mir, M., 1972).

[4]A. A. Samokhvalov, in: Redkozemel'nye poluprovodniki (Rare-Earth Semiconductors), Nauka, L., 1977.

[5]V. A. Kapustin, in: Redkozemel'nye poluprovodniki (Rare-Earth Semiconductors), Nauka, L., 1977.

[6]É. L. Nagaev, Usp. Fiz. Nauk 117, 437 (1975) [Sov. Phys. Usp. 18, 863 (1975)].

[7]A. V. Golubkov, E. V. Goncharova, V. P. Zhuze, and I. G. Manoǐlova, Fiz. Tverd. Tela (Leningrad) 7, 2430 (1965) [Sov. Phys. Solid State 7, 1963 (1966)].

[8]A. V. Golubkov, E. V. Goncharova, V. P. Zhuze, and I. G. Manoǐlova, in: Khal'kogenidy (Chalcogenides), Naukova Dumka, Kiev, 1967, p. 141.

[9]V. P. Zhuze, A. V. Golubkov, E. V. Goncharova, T. I. Komarova, and V. M. Sergeeva, Fiz. Tverd. Tela (Leningrad) 6, 268 (1964) [Sov. Phys. Solid State 6, 213 (1964)].

[10]V. M. Sergeeva, Avtoreferat kandidatskoǐ dissertatsii (Author's Abstract of Thesis for Candidate's Degree), Leningrad State University, 1972.

[11]R. Didchenko and F. P. Gortsema, J. Phys. Chem. Solids 24, 863 (1963).

[12]J. W. McClure, J. Phys. Chem. Solids 24, 871 (1963).

[13]F. J. Reid, L. K. Matson, J. F. Miller, and R. C. Himes, J. Phys. Chem. Solids 25, 969 (1964); J. Electrochem. Soc. 111, 943 (1964).

[14]V. P. Zhuze, E. V. Goncharova, N. F. Kartenko, T. I. Komarova, L. S. Parfeneva, V. M. Sergeeva, and I. A. Smirnov, Phys. Status Solidi A 18, 63 (1973).

[15]V. M. Sergeeva, E. V. Goncharova, N. F. Kartenko, M. A. Demina, I. A. Smirnov, A. I. Andryushin, and Yu. K. Misyurev, Izv. Akad. Nauk SSSR Neorg. Mater. 8, 2114 (1972).

[16]É. L. Nagaev, in: Redkozemel'nye poluprovodniki (Rare-Earth Semiconductors), Nauka, L., 1977.

[17]F. Mehran, J. B. Torrance, and F. Holtzberg, Phys. Rev. B 8, 1268 (1973).

[18]J. B. Torrance, F. Holtzberg, and T. R. McGuire, AIP Conf. Proc. No. 10, 1279 (1972).

[19]M. I. Nathan, F. Holtzberg, J. E. Smith Jr., J. B. Torrance, and J. C. Tsang, Phys. Rev. Lett. 34, 467 (1975).

[20]R. J. Birgeneau and S. M. Shapiro, in: Abstracts of Intern. Conf. on Valence Instability and Related Narrow Band Phenomena, Rochester, N. Y., 1976, p. 3.

[21]S. M. Shapiro, R. J. Birgeneau, and E. Bucher, Phys. Rev. Lett. 34, 470 (1975).

[22]A. Jayaraman, V. Narayanamurti, E. Bucher, and R. G. Maines, Phys. Rev. Lett. 25, 1430 (1970).

[23]A. Jayaraman, in: Proc. Eleventh Conf. on Rare Earth Research, Traverse City, Mich., 1974, publ. by US Atomic Energy Commision, Oak Ridge, Tennessee (1974), p. 830.

[24]B. Alascio and A. López, Solid State Commun. 14, 321 (1974).

[25]B. Alascio, Solid State Commun. 16, 717 (1975).

[26]M. Avignon and S. K. Ghatak, Solid State Commun. 16, 1243 (1975).

[27]M. Avignon and S. K. Ghatak, in: Abstracts of Intern. Conf. on Valence Instability and Related Narrow Band Phenomena, Rochester, N. Y., 1976, p. 6.

[28]M. Avignon, J. M. D. Coey, and S. K. Ghatak, Bull. Am. Phys. Soc. 20, 383 (1975).

[29]M. Avignon, S. K. Ghatak, and J. M. D. Coey, in: Abstracts of Discussion Meeting on Magnetic Semiconductors, Jülich, West Germany, 1975, p. 37.

[30]S. K. Ghatak, M. Avignon, and K. H. Bennemann, J. Phys. (Paris) 37, Suppl. C4, 289 (1976).

[31]C. A. Balseiro and A. Lopez, Solid State Commun. 17, 1241 (1975).

[32]C. A. Balseiro, M. Passeggi, and B. Alascio, Solid State Commun. 16, 737 (1975).

[33]M. Barma, T. A. Kaplan, and S. D. Mahanti, Phys. Lett. A 57, 168 (1976).

[34]M. Barma, T. A. Kaplan, and S. D. Manhanti, in: Abstracts of Intern. Conf. on Valence Instability and Related Narrow Band Phenomena, Rochester, N. Y., 1976, p. 7.

[35]A. Bringer, Z. Phys. B 21, 21 (1975).

[36]A. Bringer, in: Abstracts of Discussion Meeting on Magnetic Semiconductors, Jülich, West Germany, 1975, p. 34.

[37]S. T. Chui, Phys. Rev. B 13, 2066 (1976).

[38]J. R. Iglesias-Sicardi, A. D. Bhattacharjee, R. Tournier, B. Coqblin, and R. Jullien, in: Proc. Eleventh Conf. on Rare Earth Research, Traverse City, Mich., 1974, publ. by US Atomic Energy Commission, Oak Ridge, Tennessee (1974), p. 593.

[39]B. Coqblin, A. K. Bhattacharjee, B. Cornut, J. R. Iglesias-Sicardi, and R. Jullien, in: Abstracts of Discussion Meeting on Magnetic Semiconductors, Jülich, West Germany, 1975, p. 33.

[40]H. L. Davis, in: Proc. Ninth Conf. on Rare Earth Research, Blacksburg, West Virginia, 1971, publ. by Virginia Polytechnic Institute and State University, Blacksburg, West Virginia, 1971, p. 3.

[41]S. K. Ghatak, in: Proc. Second Intern. Conf. on Phonon Scattering, Nottingham, England, 1975, publ. by Plenum Press, New York (1976), p. 305.

[42]C. E. T. Goncalves da Silva and L. M. Falicov, Solid State Commun. 17, 1521 (1975).

[43]J. F. Herbst, R. E. Watson, and J. W. Wilkins, Solid State Commun. 13, 1771 (1973).

[44]L. L. Hirst, Phys. Kondens. Mater. 11, 255 (1970).

[45]L. L. Hirst, J. Phys. Chem. Solids 35, 1285 (1974).

[46]L. L. Hirst, in: Abstracts of Discussion Meeting on Magnetic Semiconductors, Jülich, West Germany, 1975, p. 36.

[47]L. L. Hirst, in: Abstract of Discussion Meeting on Magnetic Semiconductors, Jülich, West Germany, 1975, p. 2.

[48]L. L. Hirst, Phys. Rev. Lett. 35, 1394 (1975).

[49]J. R. Iglesias-Sicardi, A. K. Bhattacharjee, R. Jullien, and B. Coqblin, Solid State Commun. 16, 499 (1975).

[50]J. H. Jefferson, Phys. Lett. A 54, 203 (1975).

[51]J. H. Jefferson, J. Phys. C 9, 269 (1976).

[52]J. H. Jefferson and K. H. W. Stevens, J. Phys. C 9, 2151 (1976).

[53]J. H. Jefferson, in: Abstracts of Intern. Conf. on Valence Instability and Related Narrow Band Phenomena, Rochester,

N. Y., 1976, p. 8.

[54]T. A. Kaplan and S. D. Mahanti, Phys. Lett. A **51**, 265 (1975).

[55]T. A. Kaplan, S. D. Mahanti, and M. Barma, Bull. Am. Phys. Soc. **20**, 383 (1975).

[56]T. A. Kaplan, in: Abstracts of Intern. Conf. on Valence Instability and Related Narrow Band Phenomena, Rochester, N. Y., 1976, p. 5.

[57]T. Kasuya, J. Phys. (Paris) **37**, Suppl. C4 261 (1976).

[58]D. I. Khomskii and A. N. Kocharjan, Solid State Commun. **18**, 985 (1976).

[59]A. N. Kocharyan and D. I. Khomskiĭ, Zh. Eksp. Teor. Fiz. **71**, 767 (1976) [Sov. Phys. JETP **44**, 404 (1976)].

[60]S. D. Mahanti, T. A. Kaplan, and M. Barma, in: Abstracts of Twenty-First Ann. Conf. on Magnetism and Magnetic Materials, Philadelphia, 1975, Abstract 2E-3.

[61]S. D. Mahanti, T. A. Kaplan, and M. Barma, Phys. Lett. A **58**, 43 (1976).

[62]N. F. Mott, Philos. Mag. **30**, 403 (1974).

[63]T. Penney and R. L. Melcher, J. Phys. (Paris) **37**, Suppl. C4, 275 (1976).

[64]T. Penney, in: Abstracts of Intern. Conf. on Valence Instability and Related Narrow Band Phenomena, Rochester, N. Y., 1976, p. 3.

[65]D. Sherrington and P. S. Riseborough, J. Phys. (Paris) **37**, Suppl. C4, 255 (1976).

[66]P. S. Riseborough, in: Abstracts of Intern. Conf. on Valence Instability and Related Narrow Band Phenomena, Rochester, N. Y., 1976, p. 7.

[67]V. S. Oskotskiĭ and L. N. Vasil'ev, in: Tezisy I Vsesoyuznoĭ konferentsii po fizike i khimii redkozemel'nykh poluprovodnikov (Abstracts of First All-Union Conf. on the Physics and Chemistry of Rare-Earth Semiconductors), AN SSSR, Leningrad, 1976, p. 64.

[68]A. Rosengren and B. Johansson, Phys. Rev. B **13**, 1468 (1976).

[69]J. W. Schweitzer, in: Abstracts of Twenty-First Ann. Conf. on Magnetism and Magnetic Materials, Philadelphia, 1975, Abstract 2E-4.

[70]J. W. Schweitzer, Phys. Rev. B **13**, 3506 (1976).

[71]D. Sherrington and S. von Molnar, Solid State Commun. **16**, 1347 (1975).

[72]K. W. H. Stevens, J. Phys. C **5**, 1360 (1972).

[73]K. W. H. Stevens, J. Phys. C **9**, 1417 (1976).

[74]C. M. Varma and V. Heine, Phys. Rev. B **11**, 4763 (1975).

[75]C. M. Varma, Rev. Mod. Phys. **42**, 219 (1976).

[76]C. M. Varma and Y. Yafet, Phys. Rev. B **13**, 2950 (1976).

[77]H. S. Wio, B. Alascio, and A. López, Solid State Commun. **15**, 1933 (1974).

[78]D. K. Wohlleben and B. R. Coles, in: Magnetism (ed. by G. T. Rado and H. Suhl), Vol. 5, Academic Press, New York, 1973, p. 3.

[79]D. K. Wohlleben, J. Phys. (Paris) **37**, Suppl. C4 231 (1976).

[80]E. S. Alekseev and A. F. Barabanov, Fiz. Tverd. Tela (Leningrad) **18**, 1686 (1976) [Sov. Phys. Solid State **18**, 979 (1976)].

[81]A. Jayaraman, P. D. Dernier, and L. D. Longinotti, High Temp.-High Press. **7**, 1 (1975).

[82]S. von Molnar, T. Penney, and F. Holtzberg, J. Phys. (Paris) **37**, Suppl. C4, 241 (1976).

[83]G. Güntherodt, Festkörperprobleme **16**, 95 (1976).

[84]V. S. Oskotskiĭ and I. A. Smirnov, in: Redkozemel'nye poluprovodniki (Rare-Earth Semiconductors), Nauka, L., 1977.

[85]S. D. Bader, N. E. Phillips, and D. B. McWhan, Phys. Rev. B **7**, 4686 (1973).

[86]R. G. Breckenridge, A. J. Darnell, and N. C. Miller, in: Proc. Tenth Conf. on Rare Earth Research, Carefree, Arizona, 1973, publ. by U. S. Atomic Energy Commision, Oak Ridge, Tenn., 1973, p. 200.

[87]E. Bucher, V. Narayanamurti, and A. Jayaraman, J. Appl. Phys. **42**, 1741 (1971).

[88]E. Bucher, D. B. McWhan, R. G. Maines, and A. Jayaraman, Helv. Phys. Acta **45**, 2 (1972).

[89]A. Chatterjee, A. K. Singh, and A. Jayaraman, Phys. Rev. B **6**, 2285 (1972).

[90]A. Chatterjee, A. Jayaraman, S. Ramaseshan, and A. K. Singh, Acta Crystallogr. Sect. A **28**, Suppl., S243 (1972).

[91]A. Jayaraman, Indian J. Pure Appl. Phys. **9**, 983 (1971).

[92]A. Jayaraman, V. Narayanamurti, E. Bucher, J. L. Kirk, and K. Vedam, in: I. Vsesoyuznaya konferentsiya po fazovym perekhodam metalldiélektrik (sbornik kratkikh soderzhaniĭ dokladov) [First All-Union Conf. on Metal—Insulator Phase Transitions (Summaries of Papers)], Moscow State University, 1972, p. 50.

[93]A. Jayaraman, A. K. Singh, A. Chatterjee, and S. Usha Devi, Phys. Rev. B **9**, 2513 (1974).

[94]J. L. Kirk, K. Vedam, V. Narayanamurti, A. Jayaraman, and E. Bucher, Phys. Rev. B **6**, 3023 (1972).

[95]T. G. Ramesh and V. Shubba, Solid State Commun. **19**, 591 (1976).

[96]A. K. Singh, A. Jayaraman, A. Chatterjee, and S. Ramaseshan, in: Proc. Ninth Conf. on Rare Earth Research, Blacksburg, West Virginia, 1971, publ. by Virginia Polytechnic Institute and State University, Blacksburg, West Virginia, 1971, p. 360.

[97]T. L. Bzhalava, M. L. Shubnikov, S. G. Shul'man, A. V. Golubkov, and I. A. Smirnov, Fiz. Tverd. Tela (Leningrad) **18**, 3148 (1976) [Sov. Phys. Solid State **18**, 1838 (1976)].

[98]E. Yu. Tonkov and I. L. Aptekar', Fiz. Tverd. Tela (Leningrad) **16**, 1507 (1974) [Sov. Phys. Solid State **16**, 972 (1974)].

[99]T. L. Bzhalava, I. A. Smirnov, and S. G. Shul'man, in: Tezisy V. Mezhdunarodnoĭ konferentsii po fizike i tekhnike vysokikh davlenii (Abstracts of Fifth Intern. Conf. on Physics and Technology of High Pressures), Nauka, M., 1975, p. 112.

[100]T. L. Bzhalava, T. B. Zhukova, I. A. Smirnov, S. G. Shul'man, and N. A. Yakovleva, Fiz. Tverd. Tela (Leningrad) **16**, 3730 (1974) [Sov. Phys. Solid State **16**, 2428 (1975)].

[101]T. I. Volkonskaya, A. I. Shelykh, T. L. Bzhalava, S. G. Shul'man, T. B. Zhukova, and I. A. Smirnov, Fiz. Tverd. Tela (Leningrad) **17**, 1172 (1975) [Sov. Phys. Solid State **17**, 751 (1975)].

[102]E. V. Goncharova, V. S. Oskotskiĭ, T. L. Bzhalava, M. V. Romanova, and I. A. Smirnov, Fiz. Tverd. Tela (Leningrad) **18**, 2065 (1976) [Sov. Phys. Solid State **18**, 1201 (1976)].

[103]A. I. Grachev, A. A. Kukharskiĭ, V. V. Kaminskiĭ, S. V. Pogarev, I. A. Smirnov, and S. G. Shul'man, Pis'ma Zh. Tekh. Fiz. **2**, 628 (1976) [Sov. Tech. Phys. Lett. **2**, 246 (1976)].

[104]T. B. Zhukova, S. V. Pogarev, and I. A. Smirnov, in: Tezisy I Vsesoyuznoĭ konferentsii po fizike i khimii redkozemel'nykh poluprovodnikov (Abstracts of First All-Union Conf. on the Physics and Chemistry of Rare-Earth Semiconductors), AN SSSR, L., 1976, p. 70.

[105]V. V. Kaminskiĭ, A. I. Shelykh, T. T. Dedegkaev, T. B. Zhukova, S. G. Shul'man, and A. I. Smirnov, Fiz. Tverd. Tela (Leningrad) **17**, 1546 (1975) [Sov. Phys. Solid State **17**, 1015 (1975)].

[106]V. V. Kaminskiĭ, Yu. F. Solomonov, V. E. Egorov, B. I. Smirnov, and I. A. Smirnov, Fiz. Tverd. Tela (Leningrad) **18**, 3135 (1976) [Sov. Phys. Solid State **18**, 1830 (1976)].

[107]V. V. Kaminskiĭ, B. I. Smirnov, and I. A. Smirnov, in: Tezisy I Vsesoyuznoi konferentsii po fizike i khimii redkozemel'nykh poluprovodnikov (Abstracts of First All-Union Conf. on the Physics and Chemistry of Rare-Earth Semiconductors), AN SSSR, L., 1976, p. 69.

[108]S. V. Pogarev, S. G. Shul'man, T. L. Bzhalava, and I. A. Smirnov, Fiz. Tverd. Tela (Leningrad) **18**, 243 (1976) [Sov. Phys. Solid State **18**, 140 (1976)].

[109]S. G. Shul'man, T. L. Bzhalava, T. B. Zhukova, T. T.

Dedegkaev, and I. A. Smirnov, Fiz. Tverd. Tela (Leningrad) 17, 2989 (1975) [Sov. Phys. Solid State 17, 1984 (1975)].

[110]T. L. Bzhalava, S. G. Shulman, T. T. Dedegkaev, T. B. Zhukova, and I. A. Smirnov, Phys. Lett. A 55, 161 (1975).

[111]D. W. Pohl, R. Jaggi, K. Gisler, and H. Weibel, Solid State Commun. 17, 705 (1975).

[112]I. A. Smirnov, R. Suryanarayanan, and S. G. Shulman, Phys. Status Solidi B 73, K137 (1976).

[113]I. A. Smirnov, R. S. Suryanarayanan, and S. G. Shulman, Phys. Status Solidi B 75, K153 (1976).

[114]A. I. Grachev, A. A. Kukharskiĭ, and S. G. Shul'man, in: Tezisy I Vsesoyuznoĭ konferentsii po fizike i khimii redko-zemel'nykh poluprovodnikov (Abstracts of First All-Union Conf. on the Physics and Chemistry of Rare-Earth Semi-conductors), AN SSSR, L., 1976, p. 70.

[115]A. Chenavas-Paule, P. Haen, F. Lapierre, R. Turnier, and L. Vieux-Rochas, in: Abstracts of Intern. Conf. on Valence Instability and Related Narrow Band Phenomena, Rochester, N. Y., 1976, p. 11.

[116]R. Suryanarayanan, I. A. Smirnov, G. Brun, and S. G. Shul'man, J. Phys. (Paris) 37, Suppl. C4 271 (1976).

[117]G. Busch, E. Kaldis, and P. Wachter, Helv. Phys. Acta 45, 886 (1972).

[118]B. Batlogg, A. Schlegel, and P. Wachter, J. Phys. (Paris) 37, Suppl. C4 267 (1976).

[119]B. Batlogg, E. Kaldis, A. Schlegel, and P. Wachter, Phys. Rev. B 14, 5503 (1976).

[120]E. Kaldis and P. Wachter, Solid State Commun. 11, 907 (1972).

[121]D. W. Pohl, R. Badertscher, K. A. Müller, and P. Wachter, Helv. Phys. Acta 46, 436 (1973).

[122]D. W. Pohl, R. Badertscher, K. A. Müller, and P. Wachter, Appl. Opt. 13, 95 (1974).

[123]D. W. Pohl and F. Holtzberg, Appl. Opt. 14, 1060 (1975).

[124]A. Jayaraman, E. Bucher, P. D. Dernier, and L. D. Longinotti, Phys. Rev. Lett. 31, 700 (1973).

[125]B. Cornut, F. Holtzberg, O. Penna, and J. Voiron, in: Abstracts of Intern. Conf. on Valence Instability and Related Narrow Band Phenomena, Rochester, N. Y., 1976, p. 11.

[126]R. Suryanarayanan, in: Proc. Intern. Conf. on Magnetism, Amsterdam, 1976, in: Physica (Utrecht) B and C 86-88, 227 (1977); in: Abstracts of Intern. Conf. on Valence Instability and Related Narrow Band Phenomena, Rochester, N. Y., 1976, p. 12.

[127]T. G. Ramesh and V. Shubha, in: Abstracts of Intern. Conf. on Valence Instability and Related Narrow Band Phenomena, Rochester, N. Y., 1976, p. 12.

[128]M. Campagna and S. T. Chui, Bull. Am. Phys. Soc. 20, 383 (1975).

[129]G. Chouteau, O. Pena, F. Holtzberg, T. Penney, R. Tournier, and S. von Molnar, J. Phys. (Paris) 37, Suppl. C4, 283 (1976).

[130]M. Gronau and S. Methfessel, in: Abstracts of Discussion Meeting on Magnetic Semiconductors, Jülich, West Germany, 1975, p. 42.

[131]G. Güntherodt and F. Holtzberg, Proc. Twentieth Conf. on Magnetism and Magnetic Materials, San Francisco, 1974, in: AIP Conf. Proc. No. 24, 36 (1974).

[132]G. Güntherodt and F. Holtzberg, in: Abstracts of Discussion Meeting on Magnetic Semiconductors, Jülich, West Germany, 1975, p. 39.

[133]G. Güntherodt and F. Holtzberg, Solid State Commun. 18, 181 (1976).

[134]G. Güntherodt, R. L. Melcher, T. Penney, and F. Holtzberg, J. Magn. Magn. Mater. 3, 93 (1976).

[135]F. Holtzberg, AIP Conf. Proc. No. 18, 478 (1973).

[136]F. Holtzberg, O. Penna, T. Penney, and R. Tournier, in: Abstracts of Intern. Conf. on Valence Instability and Related Narrow Band Phenomena, Rochester, N. Y., 1976, p. 10.

[137]F. Holtzberg and R. Tournier, in: Abstracts of Intern. Conf. on Valence Instability and Related Narrow Band Phe-nomena, Rochester, N. Y., 1976, p. 15.

[138]A. Jayaraman, P. Dernier, and L. D. Longinotti, Phys. Rev. B 11, 2783 (1975).

[139]Lung-jo Tao, Proc. Twentieth Conf. on Magnetism and Magnetic Materials, San Francisco, 1974, in: AIP Conf. Proc. No. 24, 33 (1974).

[140]S. von Molnar and F. Holtzberg, Proc. Twenty-First Conf. on Magnetism and Magnetic Materials, Philadelphia, 1975, in: AIP Conf. Proc. No. 29, 394 (1976).

[141]R. L. Melcher, G. Güntherodt, T. Penney, and F. Holtz-berg, Proc. Ultrasonics Symposium, Institution of Electrical Engineers, London (1975), p. 16.

[142]T. Penney and F. Holtzberg, Phys. Rev. Lett. 34, 322 (1975).

[143]T. Penney, R. L. Melcher, F. Holtzberg, and G. Güntherodt, Proc. Twenty-First Conf. on Magnetism and Magnetic Materials, Philadelphia, 1975, in: AIP Conf. Proc. No. 29, 392 (1976).

[144]J. E. Smith Jr., F. Holtzberg, M. I. Nathan, and J. C. Tsang, Proc. Third Intern. Conf. on Light Scattering in Solids, Campinas, Brazil, 1975, publ. by Flammarion Sciences, Paris; Halsted, New York (1976), p. 313.

[145]Lung-jo Tao, F. Holtzberg, and R. Tournier, Bull. Am. Phys. Soc. 19, 208 (1974).

[146]Lung-jo Tao and F. Holtzberg, Phys. Rev. B 11, 3842 (1975).

[147]J. C. Tsang, F. Holtzberg, M. I. Nathan, and J. E. Smith Jr., Bull. Am. Phys. Soc. 20, 378 (1975).

[148]J. C. Tsang, Solid State Commun. 18, 57 (1976).

[149]W. M. Walsh Jr., L. W. Rupp Jr., E. Bucher, and L. D. Longinotti, AIP Conf. Proc. No. 18, 535 (1973).

[150]A. Jayaraman, in: Abstracts of Intern. Conf. on Valence Instability and Related Narrow Band Phenomena, Rochester, N. Y., 1976, p. 3.

[151]D. Pohl, in: Abstracts of Intern. Conf. on Valence Instability and Related Narrow Band Phenomena, Rochester, N. Y., 1976, p. 3.

[152]B. A. Abdikamalov, I. L. Aptekar', V. M. Sergeeva, and E. Yu. Tonkov, Fiz. Tverd. Tela (Leningrad) 18, 2975 (1976) [Sov. Phys. Solid State 18, 1734 (1976)].

[153]I. L. Aptekar', L. G. Maĭstrenko, V. M. Polovov, V. M. Sergeeva, and E. Yu. Tonkov, Fiz. Tverd. Tela (Leningrad) 19, 1021 (1977) [Sov. Phys. Solid State 19, 594 (1977)].

[154]I. L. Aptekar', in: Tezisy I Vsesoyuznoĭ konferentsii po fizike i khimii redkozemel'nykh poluprovodnikov (Abstracts of First All-Union Conf. on the Physics and Chemistry of Rare-Earth Semiconductors), AN SSSR, Leningrad, 1976, p. 67.

[155]I. L. Aptekar', E. Yu. Tonkov, V. M. Polovov, V. I. Rashchupkin, and V. M. Sergeeva, in: Tezisy I Vsesoyuznoĭ konferentsii po fizike i khimii redkozemel'nykh poluprovodni-kov (Abstracts of First All-Union Conf. on the Physics and Chemistry of Rare-Earth Semiconductors), AN SSSR, L., 1976, p. 67.

[156]B. I. Smirnov, A. V. Golubkov, and I. A. Smirnov, Fiz. Tverd. Tela (Leningrad) 18, 2097 (1976) [Sov. Phys. Solid State 18, 1222 (1976)].

[157]E. V. Goncharova, M. V. Romanova, and V. M. Sergeeva, in: Tezisy I Vsesoyuznoĭ konferentsii po fizike i khimii red-kozemel'nykh poluprovodnikov (Abstracts of First All-Union Conf. on the Physics and Chemistry of Rare-Earth Semi-conductors), AN SSSR, L., 1976, p. 66.

[158]S. M. Shapiro, R. J. Birgeneau, D. B. McWhan, and E. Bucher, Bull. Am. Phys. Soc. 20, 383 (1975).

[159]M. B. Maple and D. Wohlleben, Phys. Rev. Lett. 27, 511 (1971).

[160]V. V. Tikhonov, A. V. Golubkov, and I. A. Smirnov, Fiz. Tverd. Tela (Leningrad) 8, 3578 (1966) [Sov. Phys. Solid State 8, 2860 (1967)].

[161]I. A. Smirnov, Phys. Status Solidi A 14, 363 (1972).

[162]E. V. Shadrichev, L. S. Parfen'eva, V. I. Tamarchenko,

138   Sov. Phys. Usp. 21(2), Feb. 1978

I. A. Smirnov and V. S. Oskotskiĭ   138

O. S. Gryaznov, V. M. Sergeeva, and I. A. Smirnov, Fiz. Tverd. Tela (Leningrad) 18, 2380 (1976) [Sov. Phys. Solid State 18, 1388 (1976)].

[163]L. S. Parfen'eva, I. A. Smirnov, and E. V. Shadrichev, in: Tezisy I Vsesoyuznoĭ konferentsii po fizike i khimii redkozemel'nykh poluprovodnikov (Abstracts of First All-Union Conf. on the Physics and Chemistry of Rare-Earth Semiconductors), AN SSSR, L., 1976, p. 72.

[164]V. E. Adamyan, A. V. Golubkov, and G. M. Loginov, Fiz. Tverd. Tela (Leningrad) 7, 301 (1965) [Sov. Phys. Solid State 7, 239 (1965)].

[165]B. Batlogg, J. Schoenes, and P. Wachter, Phys. Lett. A 49, 13 (1974).

[166]F. Holtzberg and J. B. Torrance, AIP Conf. Proc. No. 5, 860 (1971).

[167]G. V. Lashkarev and L. A. Ivanchenko, J. Non-Cryst. Solids 8–10, 670 (1972).

[168]R. Suryanarayanan, C. Paparoditis, J. Ferre, and B. Briat, Vide Suppl., xx, 637 (1970).

[169]R. Suryanarayanan, C. Paparoditis, J. Ferre, and B. Briat, J. Appl. Phys. 43, 4105 (1972).

[170]R. Suryanarayanan and G. Brun, Thin Solid Films 35, 263 (1976).

[171]K. Vedam and J. L. Kirk, in: Proc. Eleventh Conf. on Rare Earth Research, Traverse City, Mich., 1974, publ. by US Atomic Energy Commission, Oak Ridge, Tennessee (1974), p. 840.

[172]L. N. Vasil'ev and V. S. Oskotskiĭ, Fiz. Tverd. Tela (Leningrad) 18, 904 (1976) [Sov. Phys. Solid State 18, 523 (1976)].

[173]L. A. Ivanchenko, G. V. Lashkarev, Yu. B. Paderno, S. V. Drozdova, V. A. Obolonchik, E. I. Yarembash, and V. F. Gol'nik, Ukr. Fiz. Zh. 16, 510 (1971).

[174]A. A. Kukharskiĭ, I. A. Smirnov, and S. G. Shul'man, in: Tezisy I Vsesoyuznoi konferentsii po fizike i khimii redkozemel'nykh poluprovodnikov (Abstracts of First All-Union Conf. on the Physics and Chemistry of Rare-Earth Semiconductors), AN SSSR, L., 1976, p. 68.

[175]B. Batlogg and P. Wachter, in: Abstracts of Intern. Conf. on Valence Instability and Related Narrow Band Phenomena, Rochester, N. Y., 1976, p. 11.

[176]G. V. Lashkarev, L. A. Ivanchenko, V. A. Obolonchik, T. M. Mikhlina, and V. I. Lazorenko, in: Khimicheskaya svyaz' v poluprovodnikakh, Nauka i tekhnika, Minsk, 1969, p. 315 (Chemical Bonds in Solids, Vol. 4, Consultants Bureau, New York, 1972, p. 39).

[177]G. V. Lashkarev, L. A. Ivanchenko, Yu. B. Paderno, S. V. Drozdova, and V. A. Obolonchik, in: Redkozemel'nye metally, splavy i soedineniya (Rare-Earth Metals, Alloys, and Compounds), Nauka, M., 1973, p. 303.

[178]S. V. Pogarev, E. V. Goncharova, I. A. Smirnov, and T. L. Bzhalava, in: Tezisy I Vsesoyuznoi konferentsii po fizike i khimii redkozemel'nykh poluprovodnikov (Abstracts of First All-Union Conf. on the Physics and Chemistry of Rare-Earth Semiconductors), AN SSSR, L., 1976, p. 68.

[179]V. S. Oskotskiĭ, Fiz. Tverd. Tela (Leningrad) 19, 1825 (1977) [Sov. Phys. Solid State 19, 1065 (1977)].

[180]G. H. Dieke, Spectra and Energy Levels of Rare Earth Ions in Crystals, Interscience, New York, 1968.

[181]D. L. Wood and W. Kaiser, Phys. Rev. 126, 2079 (1962).

[182]E. Bucher and R. G. Maines, Solid State Commun. 11, 1441 (1972).

[183]G. Güntherodt, R. Keller, P. Grünberg, R. Merlin, W. B. Holzapfel, and F. Holtzberg, in: Abstracts of Intern. Conf. on Valence Instability and Related Narrow Band Phenomena, Rochester, N. Y., 1976, p. 15.

[184]M. B. Maple and D. Wohlleben, AIP Conf. Proc. No. 18, 447 (1973).

[185]J. M. D. Coey, S. K. Ghatak, and F. Holtzberg, Proc. Twentieth Conf. on Magnetism and Magnetic Materials, San Francisco, 1974, in: AIP Conf. Proc. No. 24, 38 (1974).

[186]J. M. D. Coey, S. K. Ghatak, M. Avignon, and F. Holtzberg, Phys. Rev. B 14, 3744 (1976).

[187]J. M. D. Coey and O. Massenet, in: Abstracts of Intern. Conf. on Valence Instability and Related Narrow Band Phenomena, Rochester, N. Y., 1976, p. 6.

[188]I. Nowik, in: Abstracts of Intern. Conf. on Valence Instability and Related Narrow Band Phenomena, Rochester, N. Y., 1976, p. 6.

[189]Yu. P. Smirnov, O. I. Sumbaev, E. V. Petrovich, V. S. Zykov, A. I. Egorov, and A. I. Grushko, Zh. Eksp. Teor. Fiz. 57, 1139 (1969) [Sov. Phys. JETP 30, 622 (1970)].

[190]E. V. Petrovich, Yu. P. Smirnov, V. S. Zykov, A. I. Grushko, O. I. Sumbaev, I. M. Band, and M. B. Trzhaskovskaya, Zh. Eksp. Teor. Fiz. 61, 1756 (1971) [Sov. Phys. JETP 34, 935 (1972)].

[191]V. A. Shaburov, A. E. Sovestnov, and O. I. Sumbaev, Pis'ma Zh. Eksp. Teor. Fiz. 18, 425 (1973) [JETP Lett. 18, 249 (1973)].

[192]V. A. Shaburov, A. E. Sovestnov, and O. I. Sumbaev, Phys. Lett. A 49, 83 (1974).

[193]V. A. Shaburov, A. I. Egorov, G. A. Krutov, A. S. Ryl'nikov, A. E. Sovestnov, and O. I. Sumbaev, Zh. Eksp. Teor. Fiz. 68, 326 (1975) [Sov. Phys. JETP 41, 158 (1975)].

[194]A. I. Grushko, A. I. Egorov, G. A. Krutov, T. B. Mezentseva, E. V. Petrovich, Yu. P. Smirnov, and O. I. Sumbaev, Zh. Eksp. Teor. Fiz. 68, 1894 (1975) [Sov. Phys. JETP 41, 949 (1975)].

[195]A. I. Egorov, E. V. Petrovich, Yu. P. Smirnov, A. E. Sovestnov, O. I. Sumbaev, and V. A. Shaburov, Izv. Akad. Nauk SSSR Ser. Fiz. 40, 395 (1976).

[196]O. I. Sumbaev, in: Tezisy I Vsesoyuznoĭ konferentsii po fizike i khimii redkozemel'nykh poluprovodnikov (Abstracts of First All-Union Conf. on the Physics and Chemistry of Rare-Earth Semiconductors), AN SSSR, L., 1976, p. 63.

[197]I. M. Band and M. B. Trzhaskovskaya, Tablitsy sobstvennykh znacheniĭ énergiĭ élektronov, plotnosteĭ vblizi nulya i srednikh znachenii v samosoglasovannykh polyakh atomov i ionov, $53 \leqslant Z \leqslant 63$ (Tables of Eigenvalues of Electron Energies, Densities Near Zero, and Average Densities in Self-Consistent Fields of Atoms and Ions, $53 \leqslant Z \leqslant 63$), Preprint No. 91, Leningrad Institute of Nuclear Physics, Academy of Sciences of the USSR, 1974.

[198]E. Bucher, M. Campagna, F. J. di Salvo, M. W. Walsh, Jr., P. D. Dernier, L. D. Longinotti, A. S. Cooper, G. W. Hull Jr., A. Jayaraman, V. V. Triplett, N. S. Dixon, P. Boolchand, S. S. Hanna, G. Long, and B. Lüthi, Abstracts of Discussion Meeting on Magnetic Semiconductors, Jülich, West Germany, 1975, p. 32.

[199]M. Campagna, E. Bucher, G. K. Wertheim, D. N. E. Buchanan, and L. D. Longinotti, in: Proc. Eleventh Conf. on Rare Earth Research, Traverse City, Mich., 1974, publ. by US Atomic Energy Commission, Oak Ridge, Tennessee (1974), p. 810.

[200]M. Campagna, E. Bucher, G. K. Wertheim, and L. D. Longinotti, Phys. Rev. Lett. 33, 165 (1974).

[201]M. Campagna, G. K. Wertheim, and E. Bucher, Proc. Twentieth Conf. on Magnetism and Magnetic Materials, San Francisco, 1974, in: AIP Conf. Proc. No. 24, 22 (1974).

[202]M. Campagna, S. T. Chui, G. K. Wertheim, L. D. Longinotti, and E. Bucher, Abstracts of Discussion Meeting on Magnetic Semiconductors, Jülich, West Germany, 1975, p. 41.

[203]M. Campagna, S. T. Chui, G. K. Wertheim, and E. Tosatti, Phys. Rev. B 14, 653 (1976).

[204]D. E. Eastman, F. Holtzberg, J. Freeouf, and M. Erbudak, AIP Conf. Proc. No. 18, 1030 (1973).

[205]J. L. Freeouf, D. E. Eastman, W. D. Grobman, F. Holtzberg, and J. B. Torrance, Phys. Rev. Lett. 33, 161 (1974).

[206]W. D. Grobman, D. E. Eastman, and F. Holtzberg, Bull. Am. Phys. Soc. 18, 331 (1973).

[207]R. A. Pollak, F. Holtzberg, J. L. Freeouf, and D. E.

139   Sov. Phys. Usp. 21(2), Feb. 1978

I. A. Smirnov and V. S. Oskotskiĭ   139

Eastman, Phys. Rev. Lett. **33**, 820 (1974).

[208]M. Campagna, in: Abstracts of Intern. Conf. on Valence Instability and Related Narrow Band Phenomena, Rochester, N. Y., 1976, p. 15.

[209]L. M. Falicov and J. C. Kimball, Phys. Rev. Lett. **22**, 997 (1969).

[210]R. Ramirez and L. M. Falicov, Phys. Rev. B **3**, 2425 (1971).

[211]Rezkozemel'nye poluprovodniki. Tekushchaya bibliografi-cheskaya informatsiya (Rare-Earth Semiconductors: Current Bibliographic Data), BAN SSSR, L., Vol. 1, 1974; Vol. 2, 1975; Vols. 3 and 4, 1976; Vols. 5, 6, and 7, 1977.

Translated by A. Tybulewicz

I. A. Smirnov and V. S. Oskotskiĭ